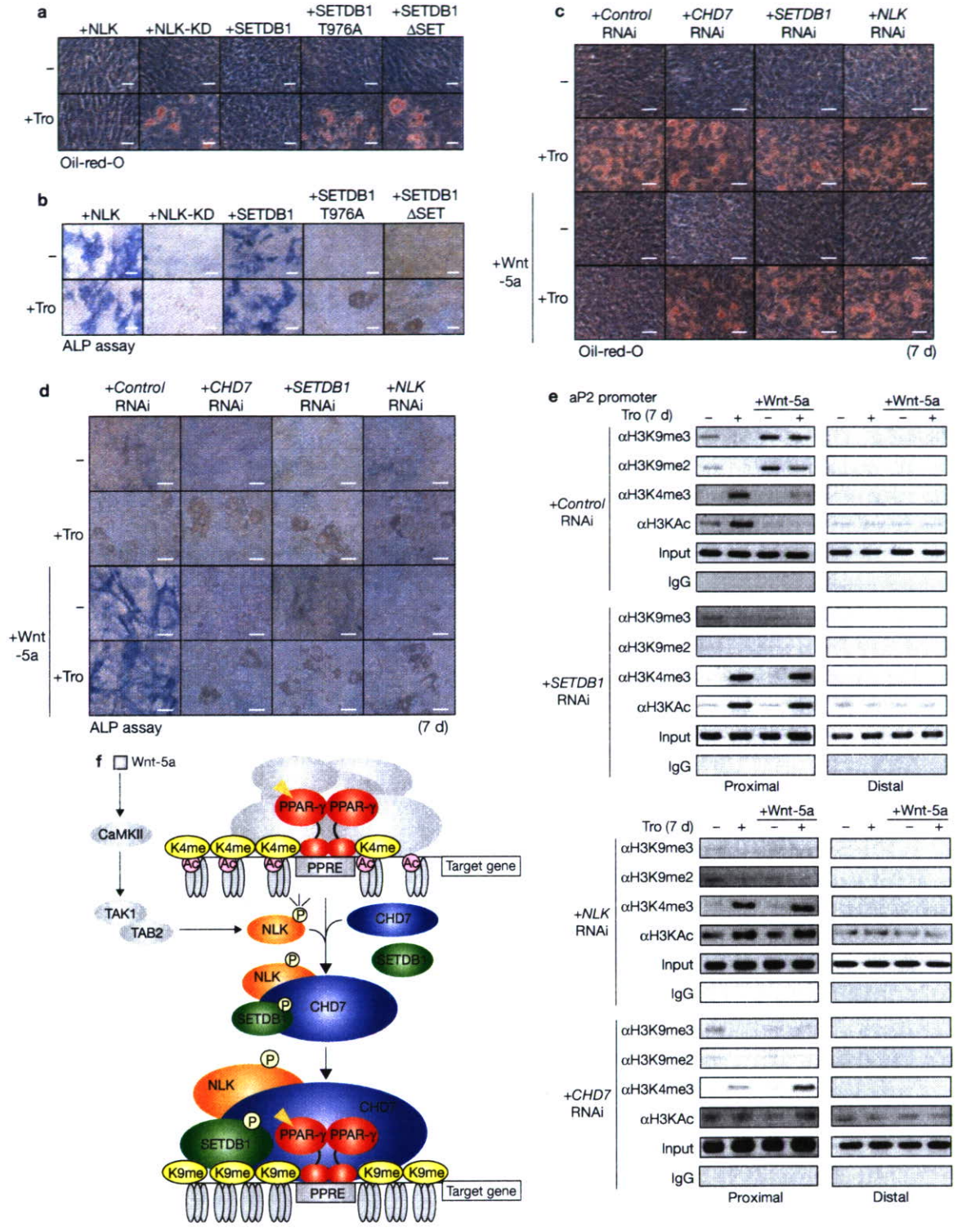

Figure 7 *NLK*, *SETDB1* and *CHD7* RNAi abrogated Wnt-5a-dependent differentiation and recruitment of modified H3. (**a**, **b**) ST2 cells overexpressed with NLK or SETDB1 mutants (NLK-KN, SETDB1T976A or SETDB1ΔSET) were incubated for 7 d, then stained with Oil-red-O (**a**) and ALP assay (**b**). Scale bars, 100 μm (**c**, **d**) *SETDB1* and *CHD7* RNAi abrogated the Wnt-5a dependent inhibition of adipogenesis. Control, *SETDB1* or *CHD7* RNAi adenovirus was infected in ST2 cells and stained with Oil-Red-O (**c**) or by ALP assay (**d**). (**e**) Chromatin immunoprecipitation analysis on aP2 promoter in ST2 cells expressing *SETDB1*, *NLK* or *CHD7* RNAi. (**f**) A mechanistic model for Wnt-5a dependent suppression of PPAR-γ function. Activated NLK through Wnt-5a-CaMKII–TAK1–TAB2 phosphorylates SETDB1. Then phosphorylated SETDB1 associates with CHD7 and act as a repressor for PPAR-γ transactivation function. CaMKII, calmodulin kinase II; PPRE, PPAR-response element; K4me, tri-methylated histone H3K4; K9me, tri-methylated histone H3K9; grey square, Wnt-5a.

© 2007 Nature Publishing Group

transrepression of PPAR-γ by Wnt-5a mediates a histone-inactivating mechanism other than histone deacetylation by a HDAC co-repressor complex. We identified an HKMT, SETDB1, as an interacting partner of activated NLK by Wnt-5a by a biochemical approach. SETDB1 seems to form a complex with CHD7 and phosphorylated NLK. However, under our purification conditions, known SETDB1 partners such as human ATFa-associated modulator (hAM) were undetectable[23]. The SETDB1 complex associated with PPAR-γ to methylate H3-K9 in the PPAR-γ target gene promoters leading to inactivation of gene expression through histone-inactivating modifications. Thus, this complex is presumed to be a new type of HKMT co-repressor complex for nuclear receptors in terms of signalling dependency. These findings are supported by a recent report that several H3-K9 HKMTs serve as co-repressors for ligand-bound nuclear receptors[44,45], although signal-induced recruitment of HKMT to nuclear receptors was not reported. In this respect, it is notable in a previous report that repression of A-Myb by activated NLK through the Wnt-1–TAK1–TAB1–HIPK2 axis was mediated by an as yet unidentified HKMT[46]. SETDB1 might be a nuclear target activated by signalling of cell-membrane receptors to co-repress several classes of transcriptional factors.

SETDB1 is shown here to be integrated into a complex through phosphorylation by activated NLK, and it then serves as a co-repressor complex component with CHD7, a platform component. Interestingly, the HKMT activity of SETDB1 required complex formation induced by the non-canonical cascade. Given that hAM is reportedly a crucial partner for forming a complex with SETDB1 that has HKMT activity and can transcriptionally repress[23], SETDB1 might be a catalytic subunit that is fully functional only when integrated into distinct protein complexes. Co-activators and co-activator complexes are required for ligand-induced transactivation of PPAR-γ, but the SETDB1–NLK–CHD7 complex seems to attenuate recruitment of such co-activators to ligand-bound PPAR-γ. In this regard, CHD7 seems to be a docking component in the complex for PPAR-γ, considering the observed interaction of CHD7 with PPAR-γ *in vitro*. Moreover, because CHD7 harbours two chromodomains that selectively recognize and preferentially bind to methylated histone lysines[39], CHD7 could also anchor this complex to specific chromosomal regions. In fact, CHD7 was revealed to selectively interact with methylated H3-K4 and H3-K9, but not acetylated histones (Fig. 5g), implicating multiple roles of CHD7 in transcriptional repression. CHD7 may target the SETDB1 complex to transcriptionally active regions through interacting with methylated H3-K4, and then SETDB1 might initiate H3-K9 methylation in the PPAR-γ target gene promoters (Fig. 7f). At the present stage, it remains unclear whether methylated H3-K4 is an initial docking signal for recruiting the SETDB1 complex or whether this complex is first recruited to PPAR-γ. Furthermore, at later stages of the repression process, through stable retention of the SETDB1 complex through interaction of CHD7 with tri-methylated H3-K9 at the promoters, the SETDB1 complex might trigger heterochromatinization from transcriptionally silent euchromatin. In this respect, CHD7, but not SETDB1, might define the target specificity of the PPAR-γ target promoters by acting as an anchor to chromatin. Likewise, other silencing factors such as DNA methyltransferase and methyl-binding protein may be recruited through CHD7 to the target promoters for stable transrepression.

For every histone modification at a specific residue, multiple histone-modifying enzymes have been identified as recognizing the same histone residue. As recent findings have shown that histone-modifying enzymes often form complexes as enzymatically functional units[45], it is conceivable that complex components enable enzymes to specifically recognize histone residues as substrates and serve as regulatory subunits that integrate with intracellular signalling. Thus, the combination of histone-modifying enzymes with their complex partners might be prerequisite for their specific roles in gene regulation at the chromatin level. □

METHODS

Plasmid construction. Expression vectors of full-length PPAR-γ, PPAR-γ mutants (S8A, S112A and S8A-S112A), TAK1, TAK1^{K63W}, C/EBPβ, GR and acyl-CoA-PPRE-tk, GRE-tk, C/EBP-RE-tk luciferase reporter vectors, GST-fusion PPAR-γs (amino acids 1–506, 1–138, 139–311, 204–506) were constructed as previously described[15]. Expression vectors of CaMKII (WT, KN and TD) and Flag–NLK and Flag–NLK^{K155M} were constructed as previously described[20]. Deletion mutants of NLK (amino acids 1–443, 124–443, 124–517) and GFP-fusion mutants of NLK were amplified by polymerase chain reaction (PCR) and cloned into pcDNA3 (Invitrogen, Carlsbad, CA) and pGEX4T-1 (Amersham, Piscataway, NJ). SETDB1 and CHD7 were cloned by PCR and inserted into pcDNA3. SETDB1ΔSET(amino acid 1–660) was cloned by PCR and inserted into pcDNA3 and SETDB1 point mutants were generated by PCR-based mutagenesis using pcDNA3-SETDB1 as a template. For GST-fusion CHD7, CHD7 constructs (amino acids 231–364) were cloned by PCR and inserted into pGEX4T-1. The expression vector of Runx2 and Runx2-RE-tk luciferase reporter vector have been previously described[17]. For luciferase assays, the DNA sequence for RNAi against β-*catenin* and *NLK* were as follows: β-*catenin*, CACGCAAGAGCAA GTAGCTGATATT; *NLK*, GAAATATCTCCATTCAGCTGGCATT.

Cell culture, Wnt-5a treatment, transfection and luciferase assays. ST2 cells were cultured and examined using Oil-red-O staining and alkaline phosphatase assays as described previously[15]. For differentiation assays, cells were treated with or without 1 μM of Tro or 50 ng ml^{-1} of recombinant Wnt-5a (R&D Systems, Minneapolis, MN) for 7 d. GPDH activity was measured using the GPDH activity measurement kit (Takara, Ohtsu, Japan). The luciferase reporter assay was performed as previously described[15].

Animal preparation. The generation of Wnt-5a$^{+/-}$, Wnt-3a$^{+/-}$ and PPAR-γ$^{+/-}$ gene-target mice was previously described[32,36,47]. These mice were crossed with C57BL6 over five generations. All experiments were performed on male mice at 18 weeks of age, and mice littermates were fed a standard diet. All mice were maintained according to the protocol approved by the Animal Care and Use Committee of the University of Tokyo.

Analysis of skeletal morphology and μ-QCT imaging. The femora were collected from 18-week old WT, Wnt-5a$^{+/-}$, Wnt-3a$^{+/-}$ and PPAR-γ$^{+/-}$ mice and fixed in 70% ethanol. Femoral bone mineral densities were determined by dual-energy X-ray absorptiometry (DCS-600EX-III, ALOKA, Tokyo, Japan). Femur bone radiographs were obtained using a soft X-ray apparatus (TRS-1005, SOFTRON, Yokohama, Japan). Histomorphometric analysis for measurement of BV/TV, trabecular number and space was conducted by the Bone Analysis Service at Kureha Special Laboratory (Tokyo, Japan). For micro-quantitative computed tomography (μ-QCT) imaging, soft tissue was meticulously removed and placed in a special polycarbonate specimen tube filled with distilled water and scanned by ScanXmate-A100S40 (Comscan techno, Yokohama, Japan). Data sets with isotropic 8.6 μm voxel spacing were acquired at 0.45° steps over a total rotation of 360° at 80 kVp. Images were reconstructed into three-dimensional volumes using true Feldkamp reconstruction with 10-bit grey levels. To determine adipocytes in bone, an upper and lower pixel intensity threshold (LUT) was chosen (110–160; adipocytes). The highlighting tool was used to select individual adipose depots for pixel counting.

RNA analysis. Total cellular RNA was isolated from ST2 cells by ISOGEN (Wako, Tokyo, Japan), and quantitative reverse transcribed PCR (RT–PCR) was performed on a TP800 sequence detector (Takara, Ohtsu, Japan). The primers used are described in the Supplementary Information. For RT–PCR analysis, RT reaction was performed using SuperScript III (Invitrogen, Carlsbad, CA), and aggrecan (amino acids 150–290) and type II collagen (amino acids 1395–1451) were amplified by PCR.

© 2007 Nature Publishing Group

Immunoprecipitation and ChIP analysis. The immunoprecipitation assay was performed as previously described[48]. For the ChIP assay, ST2 cells were incubated with or without Tro or Wnt-5a. We used the ChIP Assay Kit (Upstate, Lake Placid, NY) with antibodies against acetylated histone H3, trimethylK9H3 (Upstate), PPAR-γ, NLK (Santa Cruz Biotechnology, Santa Cruz, CA) or SETDB1 (Axxora, San Diego, CA). Antibody against CHD7 was produced by Asahi Technoglass (Funabashi, Japan). For PCR, we used the following primer pairs: 5′-AGTTC ACTAGTGGAAGTGTCACAGC-3′ (−5340 to −5315) and 5′-CTAGAAACAG ACACTGGAACCACTCT-3′ (−4800 to −4775) for aP2 gene promoter region at PPRE, and 5′-ACAGGCCTGCACAGAGGACGTTTCC-3′ (−7763 to −7739) and 5′-CATCATTTGCTATAAGTTGATTAGG-3′ (−7464 to −7439) for aP2 gene distal region. For amplification of Runx2 promoter by PCR, we used the primer pairs 5′-GGTAGAGAAGAGAGATGAAAAAGCAGAGG-3′ (−546 to −518) and 5′- GGTGTTCCTCTGTCTCTCCTTCCCT-3′ (−268 to −244) for the *Runx2* gene promoter region[49], and 5′-GCTACAATGTCGATATTCCTC-3′(−3939 to −3919) and 5′-GCATATCTGGTTGTGAGTAC-3′ (−3568 to −3549) for the *Runx2* gene distal region. Optimal PCR conditions for semi-quantitative measurement were 27 cycles of 30 s at 96 °C, 45 s at 56 °C, and 1 min at 72 °C. PCR products were visualized on 2% agarose-Tris-Acetate-EDTA (TAE) gels.

***In vitro* kinase assay and histone methylation assay.** For the *in vitro* phosphorylation assay, anti-Flag–NLK immunocomplexes were incubated with GST–SETDB1 (WT, T700A and T976A) in 10 μl of kinase buffer containing 10 mM HEPES (pH 7.4), 1 mM dithiothreitol (DTT), 5 mM $MgCl_2$ and 5 μCi of [γ^{32}P]ATP at 25 °C for 10 min. Samples were resolved by SDS polyacrylamide gel electrophoresis (SDS-PAGE), and phosphorylated proteins were visualized by imaging analyser BAS1500 (Fujifilm, Tokyo, Japan). For the histone methyltransferase assay, we used aliquots of anti-Flag–NLK immunocomplexes and the HMT assay kit (Upstate).

Protein purification. For NLK–PPAR-γ complex purification, HeLa cells stably expressing Flag–NLK were incubated with 50 mM KCl for 30 min, and nuclear extracts were prepared as previously described[37,38]. Then extracts were bound to the GST–PPAR-γ column, and complexes bound to PPAR-γ were eluted with 15 mM reduced glutathione in elution buffer (50 mM Tris-HCl, pH 8.3, 150 mM KCl, 0.5 mM EDTA, 0.5 mM PMSF, 5 mM CHD7, 0.08% NP-40 and 10% glycerol) and loaded onto an anti-Flag M2 resin column (Sigma, St Louis, MO), washed with binding buffer, and eluted by incubation for 60 min with 0.5 ml of the Flag peptide (0.2 mg ml^{-1}) (Sigma) in binding buffer. After elution, proteins were identified by MALDI-TOF mass spectroscopy (Voyager, Applied Biosystems, Foster City, CA). For glycerol density gradient fractionation, they were layered on top of a 4.5 ml linear 100%–40% glycerol gradient in the binding buffer and centrifuged for 16 h at 4 °C at 40,000 r.p.m. in a SW40 rotor (Beckman Coulter, Fullerton, CA).

Pull-down assays. NLK (amino acids 1–443, 124–517), SETDB1 (amino acids 661–1291), PPAR-γ mutants (amino acids 1–138, 139–311, 204–506, 1–506) were expressed as a GST fusion protein in *Escherichia coli* strain HB101. The expression of a protein of the predicted size was then monitored by SDS-PAGE. GST pull-down assays using [^{35}S]-methionine-labelled CHD7, $CHD7^{1-1107}$, NLK and SETDB1 were performed as previously described[15]. Peptide pull-down assays using GST–CHD7 (amino acids 231–364) were performed as previously described[50]. For histone-binding assays, GST proteins were incubated with semi-purified HeLa histones in 300 mM NaCl, 50 mM Tris-HCl (pH 7.5), 5 mM EDTA (pH 7.9), 0.5% NP40 for 2 h at room temperature. After washing three times in 500 mM NaCl, 50 mM Tris-HCl (pH 7.5), 5 mM EDTA (pH 7.9), 0.5% NP40, samples were separated by SDS-PAGE and western blotting was performed.

Adenoviral constructs and transduction. The adenoviral vector expressing RNAi against murine *NLK*, murine *SETDB1*, and murine *CHD7* were constructed from pSIREN and Adeno-X (Clontech, Palo Alto, CA). The RNAi oligonucleotide sequences are as follows: Control, CTGGACTTCCAGAAGAAATT; *NLK*, GCAGCCGTCATTACAGCAA; *SETDB1*, GGTGATGAGTACTTTGCAA; *CHD7*, GCAATCATCCCTACCTAAT. Adeno-X plasmids were digested with *PacI* and cotransfected into 293T cells using Lipofectamine Plus (Invitrogen, Carlsbad, CA). Virus-containing supernatants were collected at 48 h post-transfection and passed through a 0.45 μm filter.

Note: Supplementary Information is available on the Nature Cell Biology website.

ACKNOWLEDGEMENTS

We thank A. P. Kouzmenko, M. Kim and R. Fujiki for helpful discussions and H. Higuchi and S. Fujiyama for manuscript preparation. And we also thank S. Ishii (RIKEN Tsukuba Institute) for helpful advice and T. Komori (Nagasaki University) for the kind gift of the *Runx2* expression vector and reporter vector. This work was supported, in part, by a Grant-In-Aid for Basic Research Activities for Innovative Biosciences (BRAIN) and Priority Areas from the Ministry of Education, Science, Sports, and Culture of Japan (to S.K.).

Published online at http://www.nature.com/naturecellbiology/
Reprints and permissions information is available online at http://npg.nature.com/reprintsandpermissions

1. Fischle, W., Wang, Y. & Allis, C. D. Histone and chromatin cross-talk. *Curr. Opin. Cell Biol.* **15,** 172–183 (2003).
2. Margueron, R., Trojer, P. & Reinberg, D. The key to development: interpreting the histone code? *Curr. Opin. Genet. Dev.* **15,** 163–176 (2005).
3. Martin, C. & Zhang, Y. The diverse functions of histone lysine methylation. *Nature Rev. Mol. Cell Biol.* **6,** 838–849 (2005).
4. Bannister, A. J. & Kouzarides, T. Reversing histone methylation. *Nature* **436,** 1103–1106 (2005).
5. Metzger, E., Wissmann, M. & Schule, R. Histone demethylation and androgen-dependent transcription. *Curr. Opin. Genet. Dev.* **16,** 513–517 (2006).
6. Wu, R. C., Smith, C. L. & O'Malley, B. W. Transcriptional regulation by steroid receptor coactivator phosphorylation. *Endocr. Rev.* **26,** 393–399 (2005).
7. Dilworth, F. J. & Chambon, P. Nuclear receptors coordinate the activities of chromatin remodeling complexes and coactivators to facilitate initiation of transcription. *Oncogene* **20,** 3047–3054 (2001).
8. Rosenfeld, M. G., Lunyak, V. V. & Glass, C. K. Sensors and signals: a coactivator/corepressor/epigenetic code for integrating signal-dependent programs of transcriptional response. *Genes Dev.* **20,** 1405–1428 (2006).
9. Pascual, G. *et al.* A SUMOylation-dependent pathway mediates transrepression of inflammatory response genes by PPAR-gamma. *Nature* **437,** 759–763 (2005).
10. Evans, R. M., Barish, G. D. & Wang, Y. X. PPARs and the complex journey to obesity. *Nature Med.* **10,** 355–361 (2004).
11. Feige, J. N., Gelman, L., Michalik, L., Desvergne, B. & Wahli, W. From molecular action to physiological outputs: peroxisome proliferator-activated receptors are nuclear receptors at the crossroads of key cellular functions. *Prog. Lipid Res.* **45,** 120–159 (2006).
12. Lehrke, M. & Lazar, M. A. The many faces of PPARgamma. *Cell* **123,** 993–999 (2005).
13. Tontonoz, P., Hu, E., Graves, R. A., Budavari, A. I. & Spiegelman, B. M. mPPAR gamma 2: tissue-specific regulator of an adipocyte enhancer. *Genes Dev.* **8,** 1224–1234 (1994).
14. Hu, E., Kim, J. B., Sarraf, P. & Spiegelman, B. M. Inhibition of adipogenesis through MAP kinase-mediated phosphorylation of PPARgamma. *Science* **274,** 2100–2103 (1996).
15. Suzawa, M. *et al.* Cytokines suppress adipogenesis and PPAR-gamma function through the TAK1/TAB1/NIK cascade. *Nature Cell Biol.* **5,** 224–230 (2003).
16. Chien, K. R. & Karsenty, G. Longevity and lineages: toward the integrative biology of degenerative diseases in heart, muscle, and bone. *Cell* **120,** 533–544 (2005).
17. Harada, S. & Rodan, G. A. Control of osteoblast function and regulation of bone mass. *Nature* **423,** 349–355 (2003).
18. Ralston, S. H. & de Crombrugghe, B. Genetic regulation of bone mass and susceptibility to osteoporosis. *Genes Dev.* **20,** 2492–2506 (2006).
19. Behrens, J. *et al.* Functional interaction of beta-catenin with the transcription factor LEF-1. *Nature* **382,** 638–642 (1996).
20. Ishitani, T. *et al.* The TAK1-NLK mitogen-activated protein kinase cascade functions in the Wnt-5a/Ca(2+) pathway to antagonize Wnt/beta-catenin signaling. *Mol. Cell. Biol.* **23,** 131–139 (2003).
21. Veeman, M. T., Axelrod, J. D. & Moon, R. T. A second canon. Functions and mechanisms of beta-catenin-independent Wnt signaling. *Dev. Cell* **5,** 367–377 (2003).
22. Schultz, D. C., Ayyanathan, K., Negorev, D., Maul, G. G. & Rauscher, F. J. 3rd. SETDB1: a novel KAP-1-associated histone H3, lysine 9-specific methyltransferase that contributes to HP1-mediated silencing of euchromatic genes by KRAB zinc-finger proteins. *Genes Dev.* **16,** 919–932 (2002).
23. Wang, H. *et al.* mAM facilitates conversion by ESET of dimethyl to trimethyl lysine 9 of histone H3 to cause transcriptional repression. *Mol. Cell* **12,** 475–487 (2003).
24. Vissers, L. E. *et al.* Mutations in a new member of the chromodomain gene family cause CHARGE syndrome. *Nature Genet.* **36,** 955–957 (2004).
25. Komatsu, Y. *et al.* Targeted disruption of the Tab1 gene causes embryonic lethality and defects in cardiovascular and lung morphogenesis. *Mech. Dev.* **119,** 239–249 (2002).
26. Ishitani, T. *et al.* The TAK1-NLK-MAPK-related pathway antagonizes signalling between beta-catenin and transcription factor TCF. *Nature* **399,** 798–802 (1999).
27. Almind, K. & Kahn, C. R. Genetic determinants of energy expenditure and insulin resistance in diet-induced obesity in mice. *Diabetes* **53,** 3274–3285 (2004).
28. Mueller, E. *et al.* Terminal differentiation of human breast cancer through PPAR gamma. *Mol. Cell* **1,** 465–470 (1998).

© 2007 Nature Publishing Group

29. Hong, J. H. *et al.* TAZ, a transcriptional modulator of mesenchymal stem cell differentiation. Science **309,** 1074–1078 (2005).
30. Schwartz, A. V. *et al.* Thiazolidinedione use and bone loss in older diabetic adults. *J. Clin. Endocrinol. Metab.* **91,** 3349–3354 (2006).
31. Akune, T. *et al.* PPARgamma insufficiency enhances osteogenesis through osteoblast formation from bone marrow progenitors. *J. Clin. Invest.* **113,** 846–855 (2004).
32. Takada, S. *et al.* Wnt-3a regulates somite and tailbud formation in the mouse embryo. *Genes Dev.* **8,** 174–189 (1994).
33. Glass, D. A. 2nd *et al.* Canonical Wnt signaling in differentiated osteoblasts controls osteoclast differentiation. *Dev. Cell* **8,** 751–764 (2005).
34. Gong, Y. *et al.* LDL receptor-related protein 5 (LRP5) affects bone accrual and eye development. *Cell* **107,** 513–523 (2001).
35. Ross, S. E. *et al.* Inhibition of adipogenesis by Wnt signaling. *Science* **289,** 950–953 (2000).
36. Yamaguchi, T. P., Bradley, A., McMahon, A. P. & Jones, S. A Wnt5a pathway underlies outgrowth of multiple structures in the vertebrate embryo. *Development* **126,** 1211–1223 (1999).
37. Kitagawa, H. *et al.* The chromatin-remodeling complex WINAC targets a nuclear receptor to promoters and is impaired in Williams syndrome. *Cell* **113,** 905–917 (2003).
38. Yanagisawa, J. *et al.* Nuclear receptor function requires a TFTC-type histone acetyl transferase complex. *Mol. Cell* **9,** 553–562 (2002).
39. Brehm, A., Tufteland, K. R., Aasland, R. & Becker, P. B. The many colours of chromodomains. *Bioessays* **26,** 133–140 (2004).
40. Botrugno, O. A. *et al.* Synergy between LRH-1 and beta-catenin induces G1 cyclin-mediated cell proliferation. *Mol. Cell* **15,** 499–509 (2004).
41. Kouzmenko, A. P. *et al.* Wnt/beta-catenin and estrogen signaling converge *in vivo*. *J. Biol. Chem.* **279,** 40255–40258 (2004).
42. Asahina, M., Valenta, T., Silhankova, M., Korinek, V. & Jindra, M. Crosstalk between a nuclear receptor and beta-catenin signaling decides cell fates in the *C. elegans* somatic gonad. *Dev. Cell* **11,** 203–211 (2006).
43. Zhu, P. *et al.* Macrophage/cancer cell interactions mediate hormone resistance by a nuclear receptor derepression pathway. *Cell* **124,** 615–629 (2006).
44. Garcia-Bassets, I. *et al.* Histone methylation-dependent mechanisms impose ligand dependency for gene activation by nuclear receptors. *Cell* **128,** 505–518 (2007).
45. Wang, J. *et al.* Opposing LSD1 complexes function in developmental gene activation and repression programmes. *Nature* **446,** 882–887 (2007).
46. Kurahashi, T., Nomura, T., Kanei-Ishii, C., Shinkai, Y. & Ishii, S. The Wnt-NLK signaling pathway inhibits A-Myb activity by inhibiting the association with coactivator CBP and methylating histone H3. *Mol. Biol. Cell* **16,** 4705–4713 (2005).
47. Kubota, N. *et al.* PPAR gamma mediates high-fat diet-induced adipocyte hypertrophy and insulin resistance. *Mol. Cell* **4,** 597–609 (1999).
48. Ohtake, F. *et al.* Modulation of oestrogen receptor signalling by association with the activated dioxin receptor. *Nature* **423,** 545–550 (2003).
49. Fujiwara, M. *et al.* Isolation and characterization of the distal promoter region of mouse Cbfa1. *Biochim. Biophys. Acta* **1446,** 265–272 (1999).
50. Fujiki, R. *et al.* Ligand-induced transrepression by VDR through association of WSTF with acetylated histones. *EMBO J.* **24,** 3881–3894 (2005).

© 2007 Nature Publishing Group

nature
cell biology

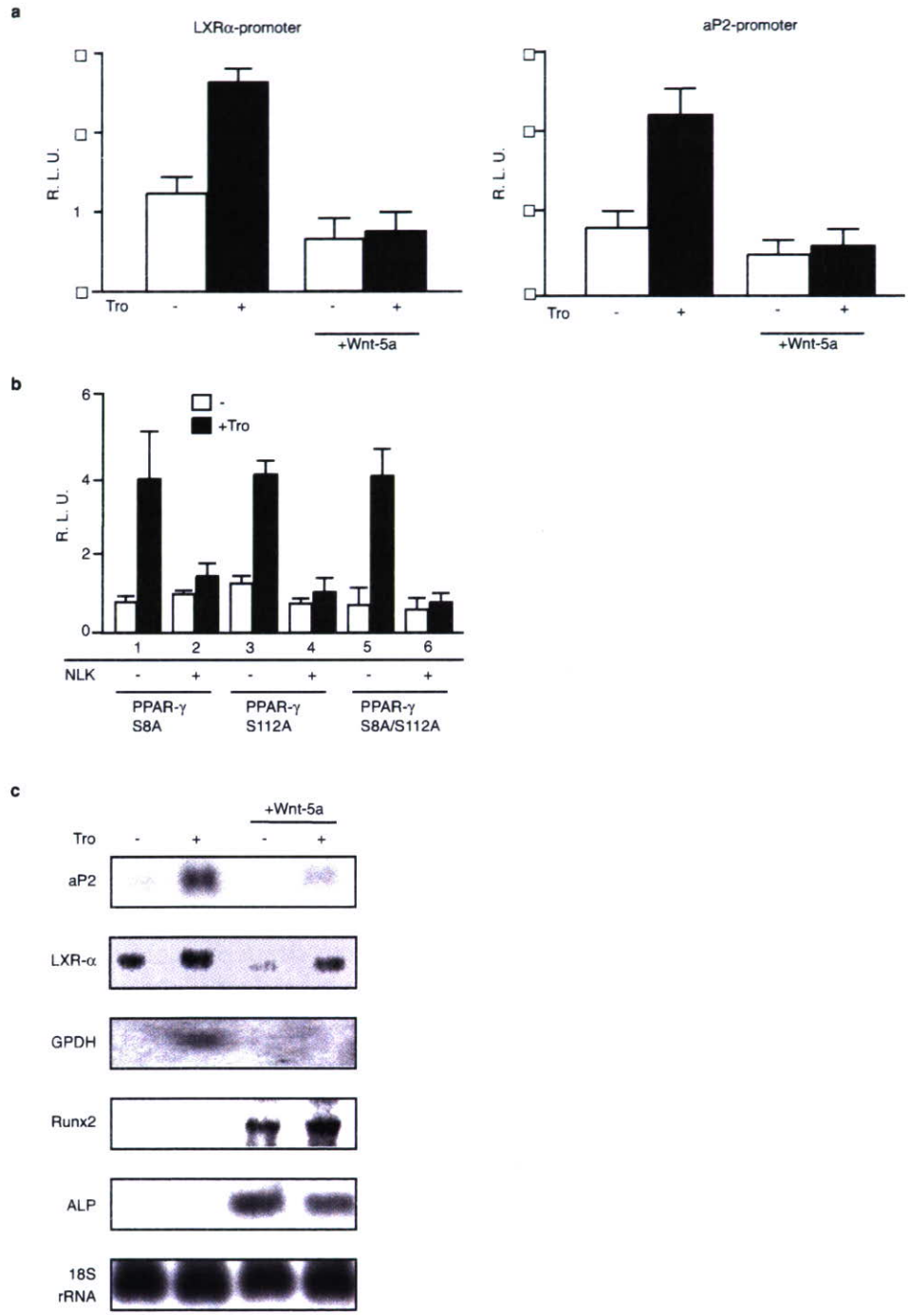

Figure S1. Supplemental data on luciferase reporter assays. (**a**) Luciferase assay in ST2 cells. After transfection with expression vectors of PPAR-γ and each reporter vectors ST2 cells were cultured with or without Wnt-5a for 24hrs and luciferase assay was performed. (**b**) Lusiferase assay in ST2 cells transfected with expression vectors of MAPK phosphorylation mutants of PPAR-γ (S8A, S112A, S8A-S112A), NLK and PPRE-tk-luc vectors. In (**a**) and (**b**), error bars represent the means +/- S. D. of triplicate, independent determinations. (**c**) Northern blot analysis for differentiation markers of adipocytes (aP2, GPDH and LXR-α) and osteoblasts (ALP and Runx2) in ST2 cells incubated with or without Wnt-5a and Tro were performed.

© 2007 Nature Publishing Group

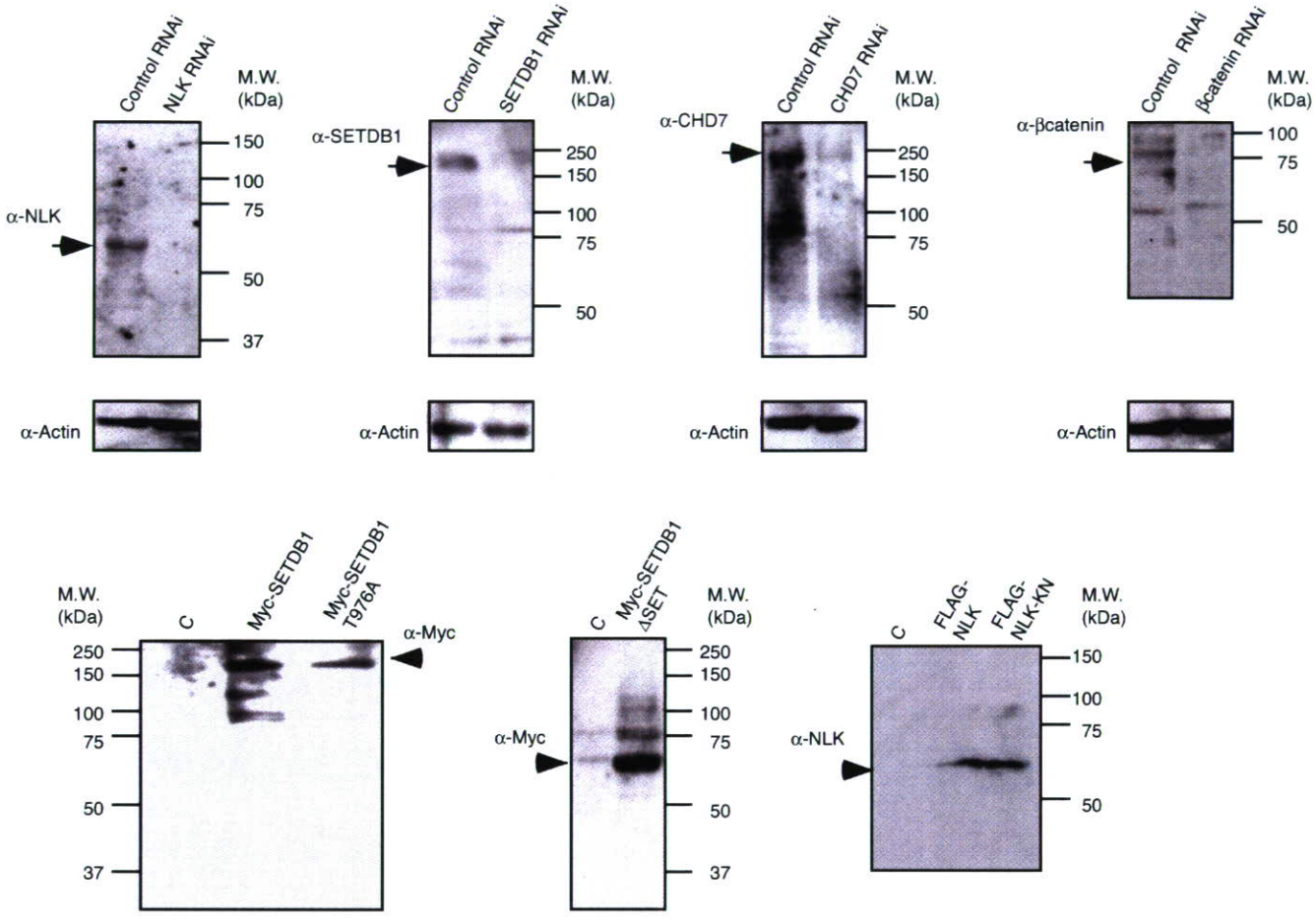

Figure S2. Supplemental data on protein expression. Each nuclear-cell extracts were prepared and then western blotting was performed.

© 2007 Nature Publishing Group

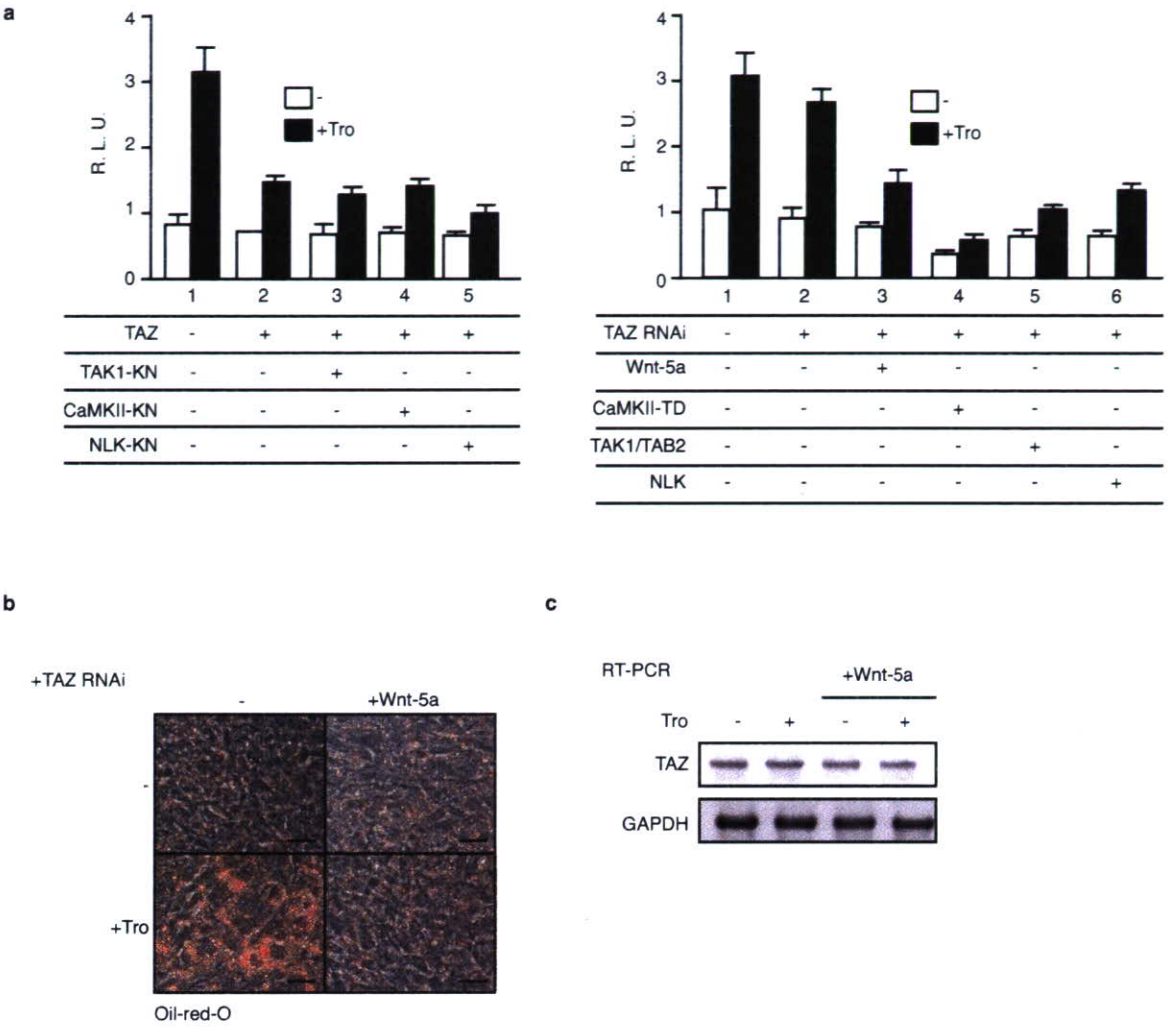

Figure S3. Supplemental data on TAZ function in Wnt-5a signaling. (**a**) Luciferase assay transfected with PPRE-tk-luc vector and indicated vectors were performed. Error bars represent the means +/- S. D. of triplicate, independent determinations. (**b**) TAZ RNAi did not abrogate Wnt-5a induced inhibition of adipogenesis. ST2 cells were transfected with adenovirus expressing mTAZ-specific RNAi and were then transferred to adipocyte differentiation medium. Cells were stained by Oil-red O. Scale bars, 100 μm. (**c**) Expression level of TAZ mRNA was not changed when treated with or without Tro or Wnt-5a in (**b**). RT-PCR was performed.

© 2007 Nature Publishing Group

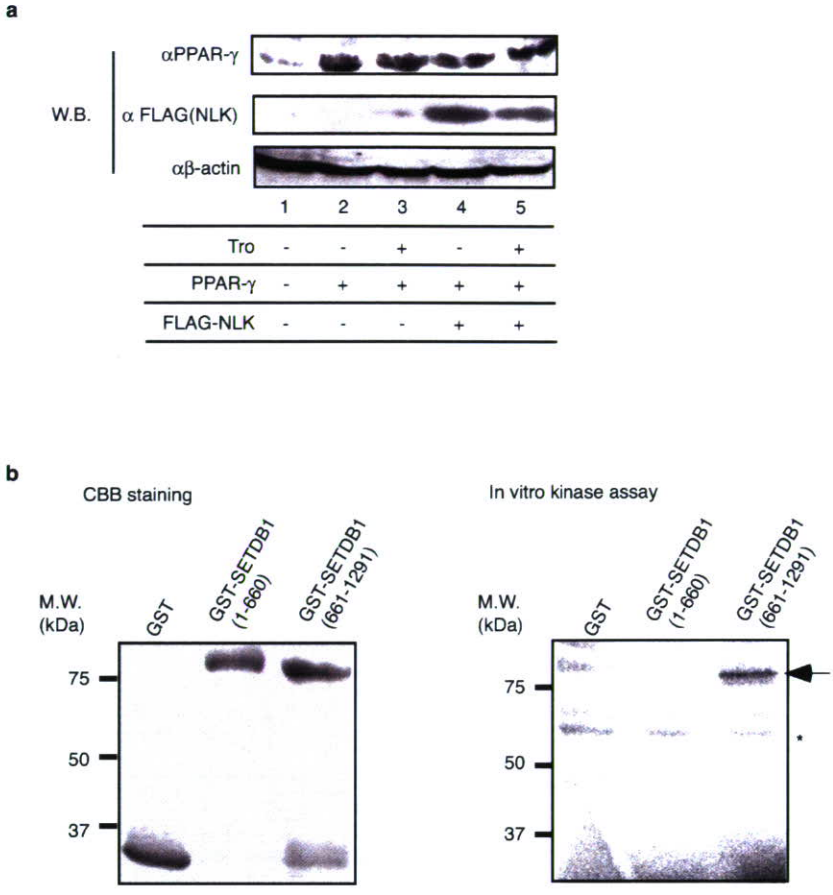

Figure S4. (a) Supplemental data on the degradation of PPAR-γ by NLK. ST2 cells were transfected with NLK expression vector and then lysates were performed for western blotting with antibody against PPAR-γ. **(b)** In vitro kinase assay using GST, GST-SETDB1 (1-660 amino aicds), and GST-SETDB1 (661-1291 amino acids). GST fused proteins were incubated with anti-FLAG-NLK immunocomplexes and [^{32}P]γ-ATP. Arrow head indicates phosphorylated GST-SETDB1 (661-1291 amino acids) and asterisk indicates self-phosphoerylated NLK.

© 2007 Nature Publishing Group

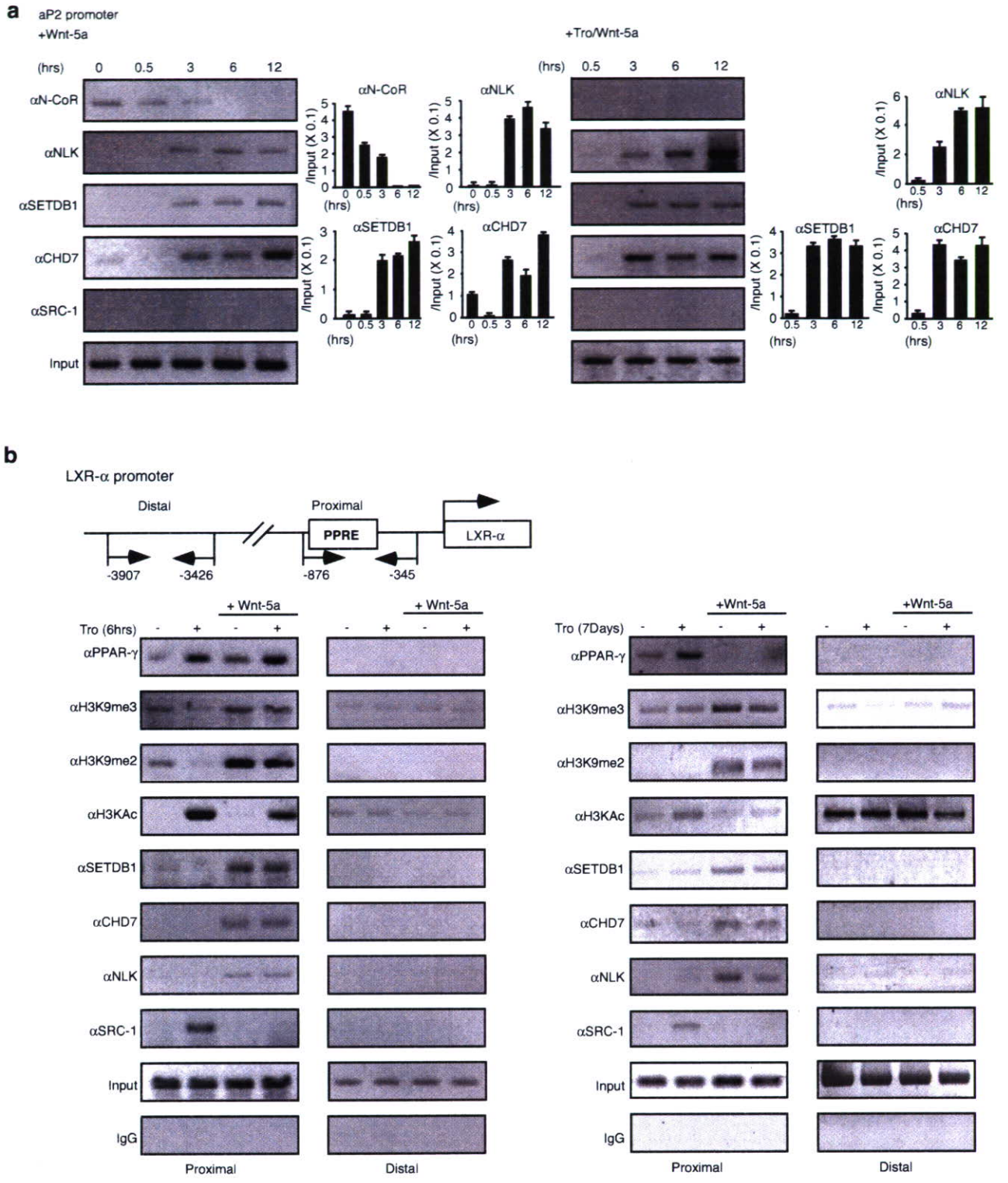

Figure S5. Supplemental data on the ChIP analysis. (**a**) Time-coursed ChIP analysis on aP2 promoter in ST2 cells. After treated with or without Tro or Wnt-5a, each time-coursed ChIP analysis was performed by using indicated antibodies. Recruitment intensity was shown as each graph. Error bars represent the means +/- S. D. of triplicate, independent determinations. (**b**) ChIP analysis on LXR-α promoter in ST2 cells. ST2 cells were treated with/without Tro and Wnt-5a for 6 hrs (left panel) or 7days (right panel). Then ChIP analysis was performed with indicated antibodies on LXR-α promoter region.

© 2007 Nature Publishing Group

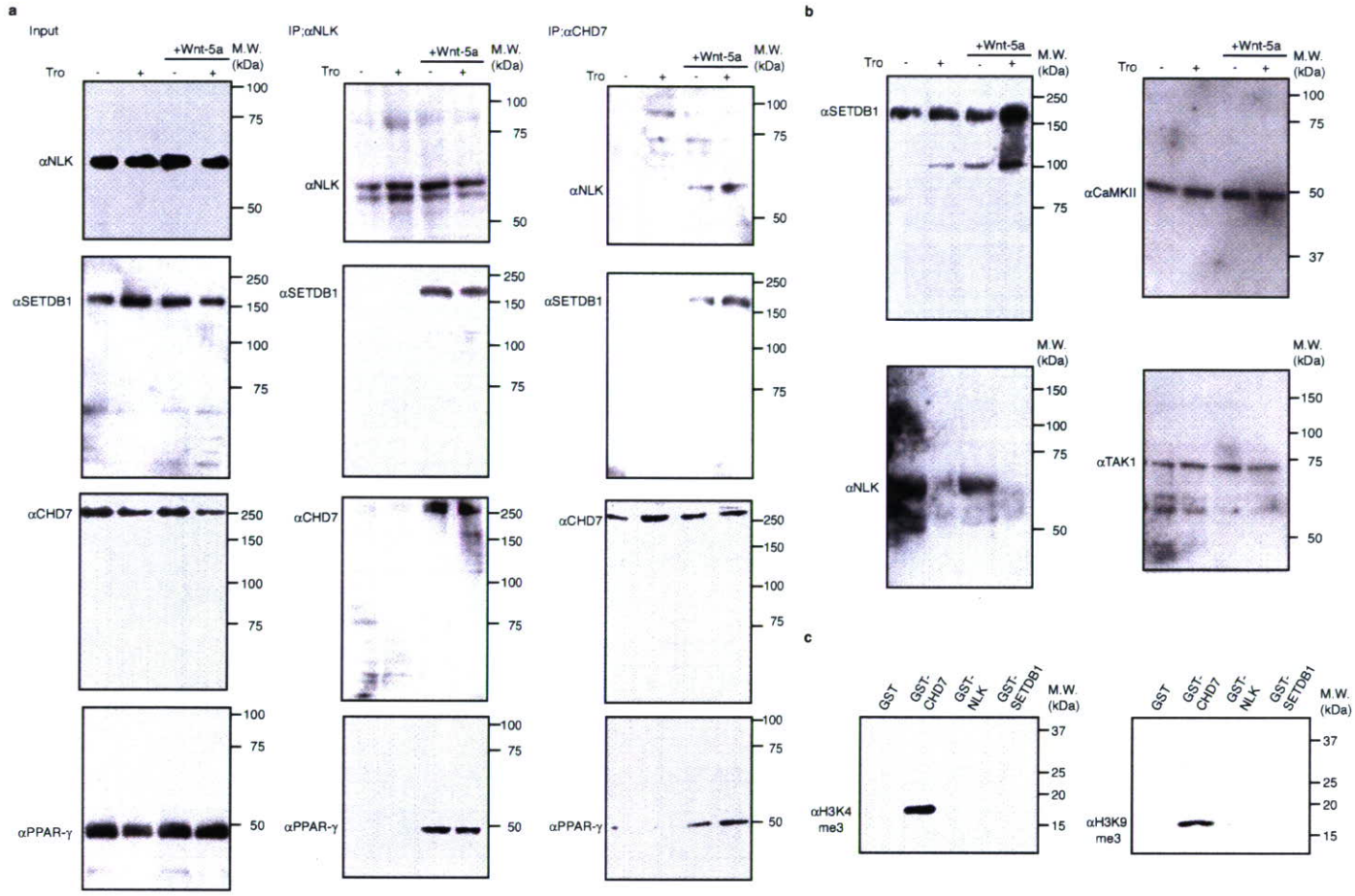

Figure S6. Selected representative full-scan images. Full sized membranes were cut prior to immunoblotting according to prestained MW markers. **(a)** Images correspond to Fig. 4e. **(b)** Images correspond to Fig. 5a left panel. **(c)** Images correspond to Fig. 5g.

Reference

1. Hong, J. H. et al. TAZ, a transcriptional modulator of mesenchymal stem cell differentiation. Science 309, 1074-8 (2005).

© 2007 Nature Publishing Group

Supplementary Information

MATERIALS

The primers used for quantitative RT-PCR were as follows;

aP2; 5'-TGGGAACCTGGAAGCTTGTCTC-3' for forward primer and 5'-GCTGATGATCATGTTGGGCTTG-3' for reverse primer.

ALP; 5'-ACACCTTGACTGTGGTTCTGCTGA-3' for forward primer and 5'-CCTTGTAGCCAGGCCCGTTA-3' for reverse primer.

Runx2; 5'-CATTTGCACTGGGTCACACGTA-3' for forward primer and 5'-GAATCTGGCCATGTTTGTGCTC-3' for reverse primer.

LXR-α; 5'-TGCAGGACCAGCTCCAAGTAGA-3' for forward primer and 5'-GGCTCACCAGCTTCATTAGCATC-3' for reverse primer.

GPDH; 5'-GGGCTGAAGCTAATCTCCGACA-3' for forward primer and 5'-AGGCCGTTCTGCTCACTTTG-3' for reverse primer.

ChIP analysis was performed as described in the text. Used primers for ChIP analysis were 5'-AGTTCAGCACAGAAGTGCTTTCCTAGC-3' (-876 to -850) and 5'-CCCATCTGAGATGGTGTCAAGATCTAC-3' (-372 to -345) for the LXR-α gene promoter region at PPRE, and 5'-CGCCCGGATGCATTCGTAAGGA-3' (-3907 to -3886) and 5'-GGCTGGTTACATGCAGTACCCT-3' (-3447 to -3426) for LXR-α gene distal region.

Reporter vectors of aP2 promoter (-4246 to -6025)-tk-luc or LXR-α promoter (-1 to

© 2007 Nature Publishing Group

-1650)-tk-luc were cloned by PCR and inserted into pGL3-tk-luc. Mouse TAZ1 cDNA was cloned by PCR and inserted into pcDNA3. RNAi sequence of TAZ1 was same as previously described[1]. Primers for RT-PCR were as follows; Fw; 5'-AATCCGTCCTCGGTGCCCCATCCGC-3', Rev; 5'-TTACAGCCAGGTTAGAAAGG-3'.

© 2007 Nature Publishing Group

The EMBO Journal (2007) 26, 764–774 | © 2007 European Molecular Biology Organization | All Rights Reserved 0261-4189/07
www.embojournal.org

THE EMBO JOURNAL

A cell cycle-dependent co-repressor mediates photoreceptor cell-specific nuclear receptor function

Shinichiro Takezawa[1,4], Atsushi Yokoyama[1], Maiko Okada[1], Ryoji Fujiki[1], Aya Iriyama[2], Yasuo Yanagi[2], Hiroaki Ito[1], Ichiro Takada[1], Masahiko Kishimoto[1], Atsushi Miyajima[1], Ken-ichi Takeyama[1], Kazuhiko Umesono[3], Hirochika Kitagawa[1] and Shigeaki Kato[1,4,*]

[1]The Institute of Molecular and Cellular Biosciences, University of Tokyo, Bunkyo-ku, Tokyo, Japan, [2]Department of Ophthalmology, University of Tokyo, School of Medicine, Bunkyo-ku, Tokyo, Japan, [3]Institute for Virus Research, and Graduate School for Biostudies, Kyoto University, Kyoto, Japan and [4]ERATO, Japan Science and Technology Agency, Kawaguchi, Saitama, Japan

Photoreceptor cell-specific nuclear receptor (PNR) (NR2E3) acts as a sequence-specific repressor that controls neuronal differentiation in the developing retina. We identified a novel PNR co-repressor, Ret-CoR, that is expressed in the developing retina and brain. Biochemical purification of Ret-CoR identified a multiprotein complex that included E2F/Myb-associated proteins, histone deacetylases (HDACs) and NCoR/HDAC complex-related components. Ret-CoR appeared to function as a platform protein for the complex, and interacted with PNR via two CoRNR motifs. Purified Ret-CoR complex exhibited HDAC activity, co-repressed PNR transrepression function *in vitro*, and co-repressed PNR function in PNR target gene promoters, presumably in the retinal progenitor cells. Notably, the appearance of Ret-CoR protein was cell-cycle-stage-dependent (from G1 to S). Therefore, Ret-CoR appears to act as a component of an HDAC co-repressor complex that supports PNR repression function in the developing retina, and may represent a co-regulator class that supports transcriptional regulator function via cell-cycle-dependent expression.

The EMBO Journal (2007) **26,** 764–774. doi:10.1038/sj.emboj.7601548; Published online 25 January 2007
Subject Categories: chromatin & transcription
Keywords: cell cycle; co-repressor complex; HDAC; PNR; retina

Introduction

Members of the nuclear receptor (NR) gene superfamily serve as sequence-specific regulators in the promoters of their cognate target genes (Mangelsdorf *et al*, 1995). Reflecting the spatiotemporal expression patterns of NRs in animals, a wide variety of biological events are under the control of NR-mediated transcriptional regulation (McKenna and O'Malley, 2002; Rosenfeld *et al*, 2006). Structurally, NR proteins can be divided into five domains, A–E. The highly conserved C domain acts as a DNA-binding domain (DBD), which has two Zn-finger motifs that recognize and stably bind to specific target DNA sequences. The moderately conserved ligand-binding domain (LBD) is mapped to the C-terminal E domain. The N-terminal A/B domain exhibits poor homology among NRs but is responsible for ligand-induced transactivation together with the LBD regions in NRs such as nuclear hormone/vitamin receptors. Unlike hormone/vitamin receptors, several NRs are believed not to require ligand binding, and are therefore classified as orphan receptors that function as ligand-independent regulators (Mangelsdorf *et al*, 1995).

Ligand-dependent and -independent transcriptional control by NRs requires histone modification and chromatin remodeling (Belandia and Parker, 2003; Kitagawa *et al*, 2003). Histone modification coupled with transcriptional control by NRs depends on the input of two types of co-regulators with opposing functions. It appears that most co-regulators exist as multiprotein complexes (McKenna and O'Malley, 2002; Perissi and Rosenfeld, 2005). It is thought that three distinct classes of co-activators support NR transactivation, with two of these classes, CBP/p160 and GCN5/TRPAP complexes (Onate *et al*, 1995; Kamei *et al*, 1996; Yanagisawa *et al*, 2002), containing histone acetyltransferase (HAT) enzymes. The other class, DRIP/TRAP complex, is a non-HAT co-activator complex (Fondell *et al*, 1996; Rachez *et al*, 1999). The co-repressor type complexes contain histone deacetylase (HDAC) enzymes, which along with NCoR/SMRT physically interact with NRs via CoRNR motifs, and are thought to be functionally indispensable subunits in NR co-repression complexes (Heinzel *et al*, 1997; Nagy *et al*, 1997). The other histone-modifying enzymes are also likely to co-regulate the NR function (Metzger *et al*, 2005). Although histone modification owing to HAT/HDAC activity in NR co-regulator complexes may in cooperation with chromatin-remodeling complexes explain at least in part the mechanism of NR-mediated transcriptional control via chromatin remodeling (Narlikar *et al*, 2002; Belandia and Parker, 2003; Kitagawa *et al*, 2003), the molecular link between NR-mediated gene regulation and cell cycle control remains elusive.

The photoreceptor-specific orphan receptor PNR (NR2E3) is a pivotal regulator in the developing retina, as it determines cone photoreceptor phenotype (Haider *et al*, 2001; Milam *et al*, 2002; Yanagi *et al*, 2002). Its significance in neuronal differentiation has been established by a number of studies based on spontaneous genetic mutations of the PNR gene in human enhanced S-cone syndrome (ESCS) patients and in

*Corresponding author. Institute of Molecular and Cellular Biosciences, University of Tokyo, Yayoi, Bunkyo-ku, Tokyo 113-0032, Japan.
Tel.: +81 3 5841 8478; Fax: +81 3 5841 8477;
E-mail: uskato@mail.ecc.u-tokyo.ac.jp

Received: 9 November 2006; accepted: 15 December 2006; published online: 25 January 2007

©2007 European Molecular Biology Organization

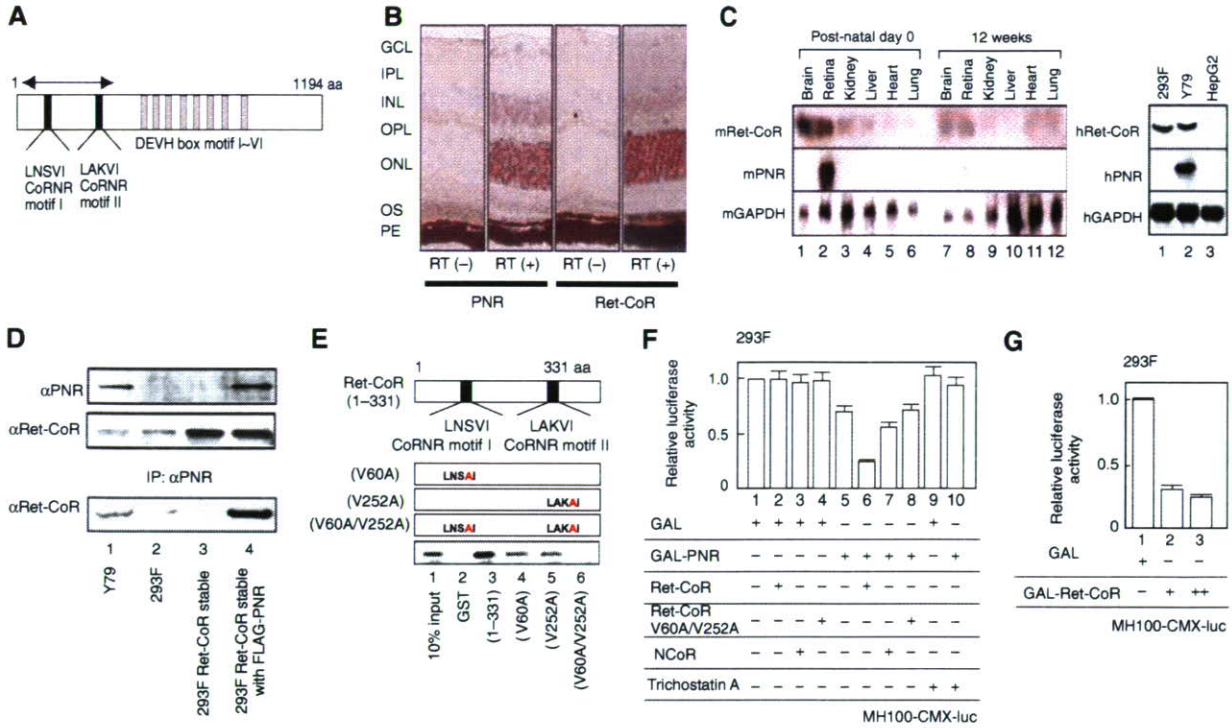

Figure 1 Identification of Ret-CoR as a novel co-repressor of an orphan nuclear receptor PNR. (**A**) Schematic diagram of Ret-CoR protein. The two CoRNR motifs, DEVH box motifs and the region corresponding to the isolated cDNA clone (arrows) by yeast two-hybrid screening are illustrated. (**B**) Expression of Ret-CoR transcripts in the retina. *In situ* RT–PCR of adult mouse retinal sections performed with [RT(+)] or without [RT(−)] reverse transcriptase (RT). PNR (left) and Ret-CoR (right) transcripts as detected by *in situ* RT–PCR are shown. GCL, ganglion cell layer; IPL, inner plexiform layer; INL, inner nuclear layer; OPL, outer nuclear layer; OS, outer segment; PE, pigment epithelium. (**C**) Expression of Ret-CoR and PNR transcripts in mouse tissue (left panel) and human culture cells (right panel) as determined by Northern blotting. (**D**) Interaction between PNR and Ret-CoR in each cell line. Whole cell extracts from Y79 cells, 293F cells, and untransfected/PNR-transfected 293F Ret-CoR stable cells were subjected to immunoprecipitation (IP) with anti-PNR antibody. Each immunoprecipitant was then analyzed by Western blot (IB) with anti-PNR or anti-Ret-CoR antibody. (**E**) The CoRNR motif of Ret-CoR mediates interaction with PNR. *In vitro*-translated PNR proteins were applied for a GST pull-down assay. (**F**) Ret-CoR mediates the co-repressive function of PNR. Luciferase assays were performed in 293F cells transfected with a GAL4-DBD-binding site × 4 containing luciferase reporter plasmid (MH100-CMX-luc) (400 ng), GAL-fused expression vectors (200 ng), Ret-CoR expression vectors (100 ng), NCoR expression vectors (100 ng) and 10^{-9} M Trichostatin A. (**G**) Ret-CoR has a transrepressive activity itself. Luciferase assays were performed as illustrated in (F) using GAL-fused Ret-CoR expression vectors (200 ng (+) or 500 ng (++)).

rd7/rd7 mice, which suffer retinal degeneration and lack color perception due to imbalanced ratio between S- and M-cone cell numbers (Akhmedov *et al*, 2000; Gerber *et al*, 2000; Haider *et al*, 2000). PNR appears to attenuate cell proliferation of S-cone cells from retinal progenitor cells, but is unlikely to control of differentiation of S into M-cone cells.

Given that the well-known NR co-repressor NCoR/SMRT was not potent to co-repress PNR (see Figure 1F), we identified a novel PNR co-repressor, designated as Ret-CoR. By a biochemical approach, Ret-CoR was shown to form an HDAC complex to co-repress PNR. Most notably, appearance of Ret-CoR protein was dependent on cell cycle. Thus, Ret-CoR may represent a novel class of co-regulators that support transcriptional function of sequence-specific regulators via cell cycle-dependent expression.

Results

Identification of Ret-CoR as a novel PNR co-repressor

We used the yeast two-hybrid system to screen a human brain cDNA library for putative co-repressors that supported the constitutive transrepression function of PNR. We identified a specific PNR-interacting clone that encoded the N-terminal region of the KIAA0890 protein (Nagase *et al*, 1998). Full-length KIAA0890 sequence encoded a 1194-amino acid-protein that contained a DEVH box motif (ATPase/helicase domain) and two CoRNR motifs (Figure 1A) that are thought to function as a physical interface for nuclear receptors and are found in co-repressors such as NCoR and SMRT (Hu and Lazar, 1999; McKenna and O'Malley, 2002). A mouse ortholog was identified from the NCBI database that showed 98% amino-acid sequence identity to human homologue. *In-situ* RT–PCR performed on slices of mouse retina revealed specific signals of this clone located at specific layers. Like expression pattern of the PNR transcript (Kobayashi *et al*, 1999), the transcript of KIAA0890 appeared to express abundantly in the outer nuclear layer (ONL) and to some extents in inner nuclear layer (INC) of the mouse retina (Figure 1B). whereas significant KIAA0890 mRNA expression was detected in mouse retina and brain tissues on postnatal day 0, levels were significantly decreased in 12-week-old mice, as determined by Northern-blot analysis (Figure 1C). The KIAA0890 gene expressed in the Y79 retinoblastoma cell line, as well as in the human embryonic renal cell line 293F, but PNR transcript was detected only in Y79 (Figure 1C, right panel). Endogenous Ret-CoR protein expression was detectable in Y79 and 293F (Figure 1C), in which nuclear localization of

©2007 European Molecular Biology Organization

Ret-CoR protein was observed (data not shown). From the expression pattern, the clone was designated as retina co-repressor (Ret-CoR) hereafter.

To investigate for interactions between PNR and Ret-CoR, we performed co-immunoprecipitation experiments on endogenous PNR and Ret-CoR proteins. Association between the proteins was observed in Y79 cells (Figure 1D), and by *in vitro* GST pull-down assay (data not shown). To map the interacting domain in Ret-CoR, *in vitro*-translated PNR and mutant Ret-CoR GST-fusion proteins were assayed. As expected from previous reports (Hu and Lazar, 1999), disruption of either CoRNR motif (V60A or V252A) in Ret-CoR significantly reduced the interaction with PNR (Figure 1E), which suggested that Ret-CoR interacts with PNR via the two CoRNR motifs.

We then tested the coregulatory function of Ret-CoR by generating a chimeric protein of PNR fused to the yeast GAL4 DNA-binding domain (DBD). A transrepressive activity was detected using the PNR-fusion protein by a transient expression assay in 293F cells (Figure 1F) and Y79 cells (data not shown). As an HDAC inhibitor trichostatin A (TSA) abrogated the transrepression by PNR (see lane 13 in Figure 1F), the HDAC activity was presumed to be required for the PNR-mediated transrepression. Ret-CoR clearly co-repressed PNR transrepression function, whereas NCoR was not so potent in 293F cells (Figure 1F) and the other cell lines (data not shown). Expectedly, TLX (NR2E1), an NR highly homologous to PNR, was also transrepressed by Ret-CoR (data not shown). Ret-CoR on its own exhibited transrepressive activity when fused with GAL4-DBD (Figure 1G). In contrast, this potentiation of transrepression was abrogated (Figure 1F) by point mutations in the Ret-CoR CoRNR motifs (see Figure 1E for the V60A/V252A mutant). Thus, our results indicated that Ret-CoR appears to serve as a co-repressor for PNR.

Ret-CoR forms an HDAC complex

To explore the molecular basis of Ret-CoR co-repressor function, we biochemically purified (Yanagisawa *et al*, 2002; Kitagawa *et al*, 2003) a Ret-CoR-containing complex. We generated stable 293F cell transformants (Ret-CoR-293F) that expressed human Ret-CoR tagged with FLAG and His epitopes at the N- and C-termini, respectively (Figure 2A). Nuclear extracts were then subjected to sequential affinity column purification using an anti-FLAG M2 affinity resin column and then a Protino Ni-affinity column. After concentrating the complexes using glycerol density gradients (Figure 2C), tagged Ret-CoR was detected in fractions that contained a complex with a molecular weight of about 1 MDa (Figure 2C). As shown in Figure 2B, middle panel, Ret-CoR appeared to form a multiprotein complex with 11 polypeptides, which were then identified by a mass spectrometry. The two background proteins appeared Hsc70 and β-actin. The complex formation and subunit identification by MALDI-TOF/MS was further confirmed by immunoprecipitation of the purified complex by an RbAp46-specific antibody (Figure 2B, right panel). Identities of these components in the glycerol density gradient functions could be further confirmed by Western blotting (see Figure 2C). The same Ret-CoR complex components were detected when the endogenous complex was immunoprecipitated of either tagged PNR or Ret-CoR from parent 293F cells by a FLAG antibody (Figure 2D). Similarly, association of endogenous PNR with endogenous complex components in Y79 could be detected by immunoprecipitation with endogenous PNR in Y79 (see Figure 3C).

The Ret-CoR complex components could be grouped into three classes based on putative function: transcription factor E2F-associated co-repressors (Sin3A, p107, HDAC1/2, RbAp48 and RbAp46 (Luo *et al*, 1998)); transcription factor Myb-associated co-repressors (NCoR (Li and McDonnell, 2002), Mybbp1A (Tavner *et al*, 1998; Fan *et al*, 2004) and CDK9 (De Falco *et al*, 2000)); and NCoR/SMRT-associated proteins (HDAC3 (Guenther *et al*, 2000)). Although TBL3 (Weinstat-Saslow *et al*, 1993) and TBL1 (Perissi *et al*, 2004) appear to share similar motif organization, the function of TBL3 has not yet been reported. Using Far Western blotting, we found that PNR interacted with Ret-CoR and CDK9, and that Ret-CoR associated with p107 and TBL3 through its N-terminal domain and with p107 and CDK9 through its C-terminal domain (Figure 2E). These interactions were further confirmed by GST-pull-down assays (Figure 2F). From these findings, we presume that Ret-CoR served as a platform protein capable of promoting assembly of various components into a Ret-CoR complex (as illustrated in Figure 7).

Appearance of the Ret-CoR protein is cell cycle-dependent

Identification of cell-cycle transcription factor-related components related to E2F (Ohtani *et al*, 1995) and Myb (Oh and Reddy, 1999) in the Ret-CoR complex led us to consider a putative role for Ret-CoR in the cell cycle. Expression of Ret-CoR through the cell cycle was investigated by Western blotting using Y79 cells synchronized by thymidine at G1/S stage and demecolcine at G2/M phase (Figure 3A). We found that like endogenous cyclin E, a marker that accumulated mostly during the G1/S transition, appearance of endogenous Ret-CoR protein was dependent on the specific cell-cycle stage from the G1 phase to the S phase (Figure 3B, left panel) when the cells were synchronized by thymidine at G1/S phase (Figure 3A, upper panel). Likewise, when the Y79 cells were synchronized by demecolcine at G2/M phase, Ret-CoR protein appearance was also cell cycle-dependent (Figure 3B, right panel). From these drug studies, the highest Ret-CoR expression (see lower panel in Figure 3B for protein levels of Ret-CoR versus Sin3A) appeared around at G1–S transition (Figure 3A, right panel). A synchronous Y79 cells also expressed Ret-CoR protein, but at low levels (Figure 3B). In the contrast, expression levels of other endogenous Ret-CoR complex components (e.g. Sin3A) and PNR proteins looked unchanged (Figure 3B). As Ret-CoR mRNA levels remained constant during the cell cycle (data not shown), the cell cycle-dependent appearance of Ret-CoR protein appears to be under post-transcriptional control, such as through protein turnover and/or translation rate. In fact, Ret-CoR protein appeared susceptible to ubiquitination for rapid degradation (Figure 3C). Consistent with the Ret-CoR protein appearance during cell cycle, association of endogenous PNR with endogenous Ret-CoR complex components was also dependent on cell cycle and most evident 4 h after G1/S arrest by thymidine (Figure 3D). These findings raised the possibility that the Ret-CoR co-repressor functions as a cell cycle-dependent repressor as well as supporting PNR transrepressive activity. This idea was further supported by the

©2007 European Molecular Biology Organization

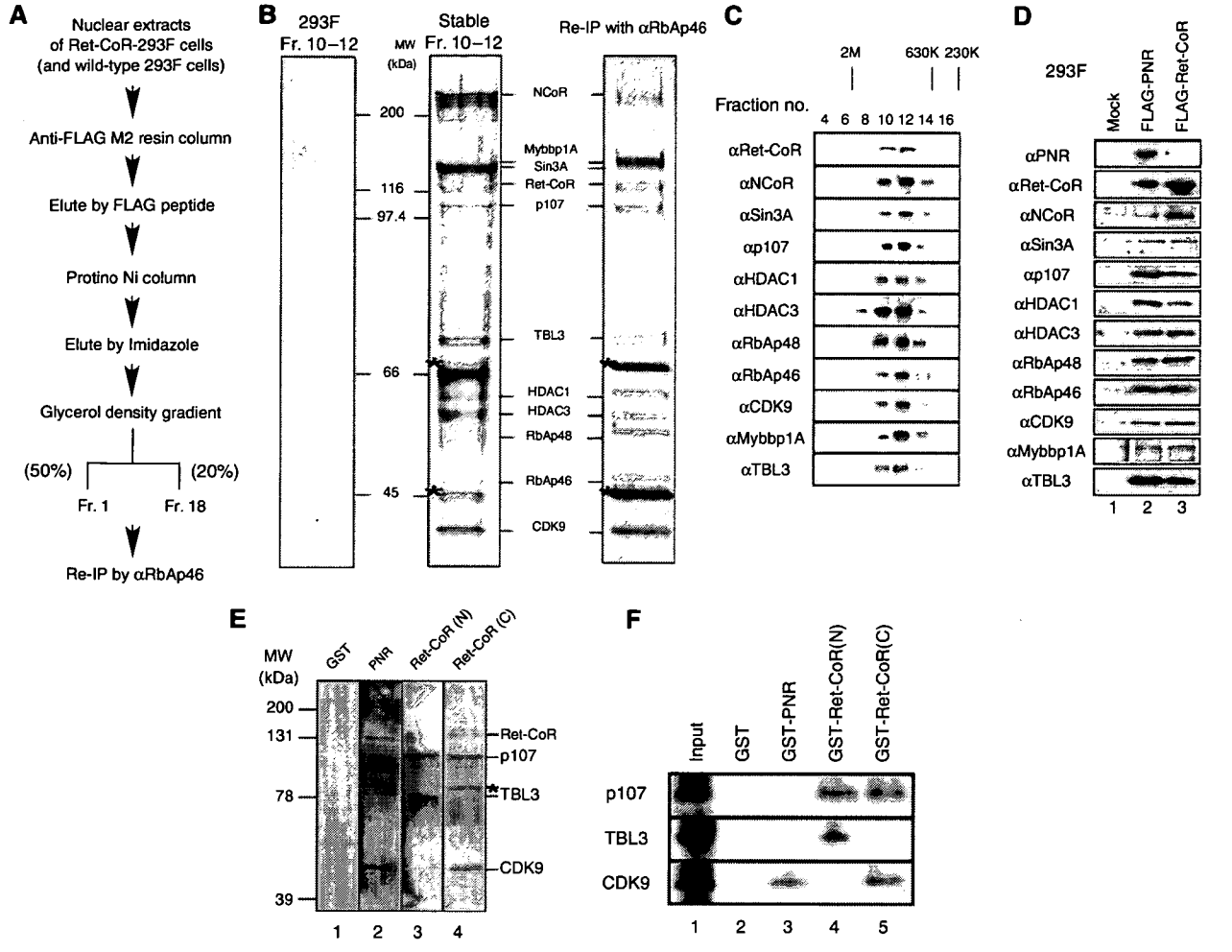

Figure 2 Identification of a novel protein complex containing Ret-CoR. (**A**) Schematic diagram of the purification for Ret-CoR-containing complex. (**B**) Mass spectrometric analysis of the purified Ret-CoR complex components. MALDI-TOF/MS analysis of the complex subunits is shown on the middle. Asterisks indicate background proteins. Silver stain of the indicated fractions of glycerol density gradient were shown at middle panel. Right panel displayed the immunoprecipitant of the purified Ret-CoR complex (middle panel) by anti-RbAp46 antibody (Pre-IP experiment). Left panel displayed immunoprecipitant of Mock cells (wild type 293F cells) precipitated by anti-FLAG M2 resin followed by the same procedure as performed with Ret-CoR complex purification. (**C**) Fractions separated by glycerol density gradient were assayed by Western blot using the indicated antibodies. (**D**) Endogenous components of Ret-CoR complex interact with tagged PNR and Ret-CoR in 293F cells. Immunoprecipitants of tagged PNR and Ret-CoR by a FLAG antibody were applied for Western blotting. (**E**) Far Western blotting of Ret-CoR complexes. Labeled probes were used, as indicated at the top of the panel. The detected bands corresponded to the proteins indicated on the right side. Asterisk indicates a background peptide. (**F**) The Ret-CoR complex components p107, TBL3 and CDK9 directly interact with PNR and Ret-CoR. *In vitro*-translated p107, TBL3 and CDK9 proteins were captured by GST-PNR, Ret-CoR N-terminal and Ret-CoR C-terminal proteins in a GST-pull down assay.

findings that co-transrepression of PNR by Ret-CoR was dependent on cell cycle stage. The PNR-mediated transcription activity was fluctuated during cell cycle and was lowered at the G1/S phase (Figure 3E), when Ret-CoR expression was high. However, by knocking down of Ret-CoR by RNAi (Supplementary Figure 1A) and an HDAC inhibitor Trichostatin A (TSA) treatment, such potent transrepressive activity of PNR at G1–S stages was abrogated (Figure 3E). Likewise, knockdown of combination of CDK9/TBL3, but not single component (only the results of several major components are displayed), resulted in clear impairment of the transrepressive PNR function even when Ret-CoR protein level was presumed high at G1–S stages through synchronization by demecolcine (Figure 3E). These findings supported again the idea that Ret-CoR serves as a co-repressor through forming an HDAC complex.

A purified Ret-CoR complex co-represses the transrepression function of PNR in vitro

To address the co-regulator function of the Ret-CoR complex on PNR, the purified Ret-CoR complex was applied to an *in vitro* transcription assay with a GAL4-DBD-fused PNR LBD chimeric protein (GAL-PNR) and a DNA template chromatinized using purified HeLa histone octamers (Kitagawa *et al*, 2003; Fujiki *et al*, 2005). A basal transcriptional activity was observed from the reporter promoter upon the binding of GAL4-DBD (GAL) alone. However, in the presence of GAL-PNR LBD, the basal activity was drastically reduced (Figure 4A, lane 2), and the addition of the purified Ret-CoR complex potently co-repressed this PNR repressor function (Figure 4A, lane 4). Reflecting the putative role of HDACs in the Ret-CoR complex in co-repression of PNR transrepression function, TSA potently attenuated the

©2007 European Molecular Biology Organization

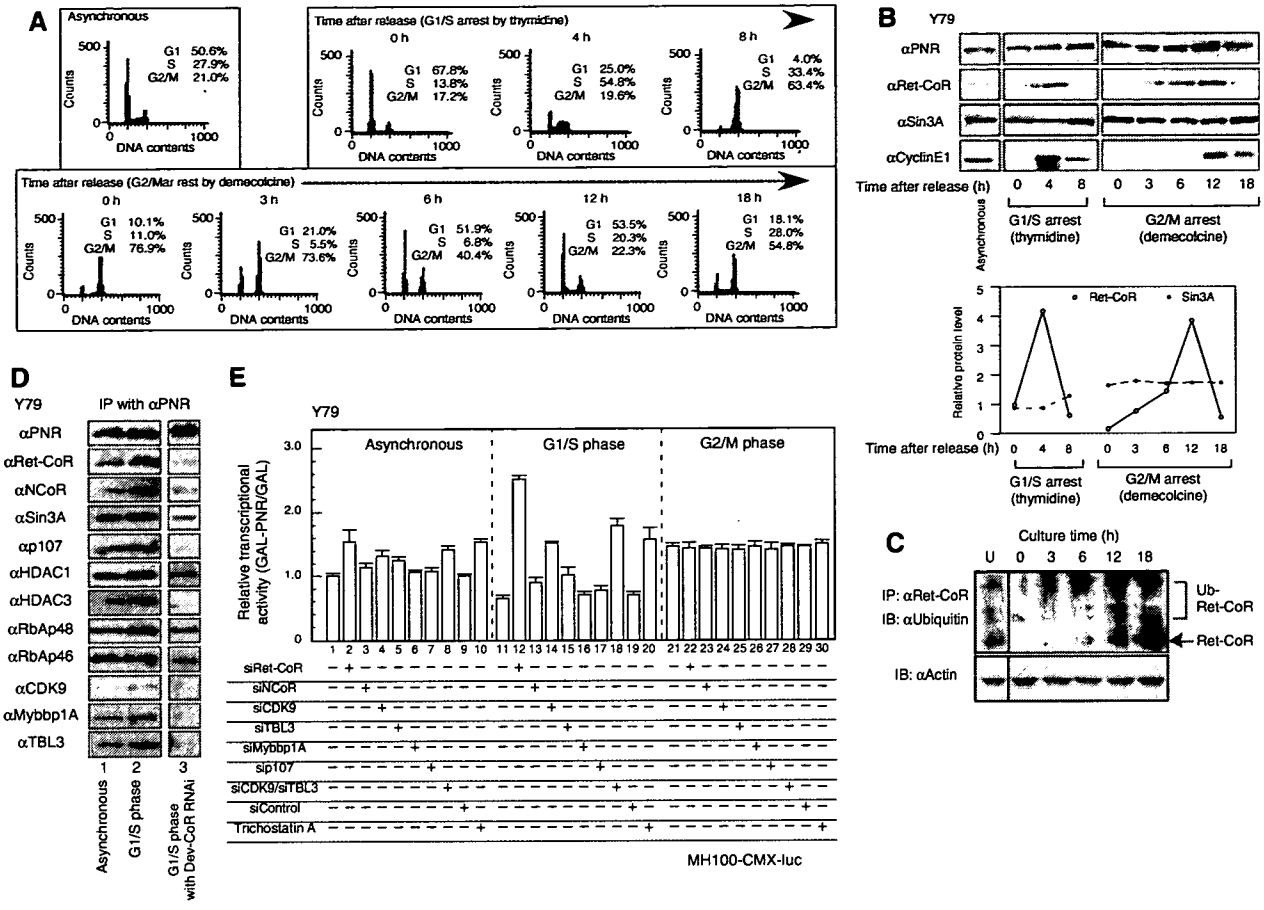

Figure 3 Funcntion of Ret-CoR containing complex is regulated by cell cycle-dependent expression of Ret-CoR. (**A**) FACS analysis of synchronized Y79 cells. Y79 cells were arrested at G1/S phase with thymidine or at G2/M phase with demecolcine. DNA contents of the cells and % populations in each synchronized culture were analyzed by FACS analysis at an indicated time after drug release. (**B**) Expression profiles of PNR and Ret-CoR through the cell cycle. Western blots shows the protein levels indicated in the panel (upper panel). Cyclin E1 was used as a G1/S transition maker. The level in the each step was quantified, normalized in asynchronous cells (lower panel; open circle, Ret-CoR; closed circle, Sin3A). (**C**) Cell cycle-dependent ubiquitination of endogenous Ret-CoR protein. Endogenous Ret-CoR was ubiquitinated in unsynchronized Y79 cells (U) and synchronized Y79 cells treated with MG132 for 3 h, and samples were taken at the indicated times after drug release. Whole cell extracts were immnoprecipitated using anti-Ret-CoR antibody and subjected to Western blotting with antibodies against indicated proteins. (**D**) Ret-CoR is required for the cell cycle-dependent interaction between endogenous Ret-CoR complex components and endogenous PNR in Y79 cells. Proteins were extracted from Y79 cells 4 h after releasing from thymidine treatment. (**E**) Cell cycle-dependent transcriptional repressive function of the Ret-CoR containing complex in Y79 cells. Luciferase assays were performed in asynchronized/synchronized Y79 cells. Relative transcriptional activity means the ratio of the GAL-PNR activity versus activity of GAL alone (GAL-PNR/GAL).

co-repressor function of the purified Ret-CoR complex (Figure 4A, lane 5). Indeed, an HDAC activity was found in the Ret-CoR immunoprecipitant (Figure 4B). When each of the complex components except Ret-CoR was knocked down by RNAi (Supplementary Figure 1A), the Ret-CoR-associated HDAC activity was not altered (Figure 4B). However, knockdown of two components (CDK9 + TBL3) caused a significant reduction in the HDAC activity like the single Ret-CoR RNAi, in accordance with the findings of co-repression of the PNR transrepressive function by the Ret-CoR complex components (Figure 3E). Thus, our findings suggested that the Ret-CoR forms an HDAC complex as a core component to co-repress PNR function.

Ret-CoR co-represses PNR function at the PNR target gene promoter cyclin D1, but not at the TBX2 promoter in Y79 cells

As shown previously in transgenic mice, proliferation in the developing retina requires cyclin D1 (Sicinski *et al*, 1995). Therefore, we reasoned that the expression of this gene, as well as that of the predicted PNR target gene TBX2 (Qian *et al*, 2005), may be under the control of both PNR and Ret-CoR. To test this hypothesis, we first measured the mRNA expression levels of cyclin D1 and TBX2 in Y79 cells by a semi-quantitative RT-PCR. Although no clear expression of cyclin D1 and TBX2 was detected in Y79 cells untransfected and transfected with a control siRNA, after knockdown of PNR expression by RNAi (Supplementary Figure 1A), significant induction of the endogenous Cyclin D1 and TBX2 genes was observed (Figure 5A, lane 2). Ret-CoR RNAi also effectively induced the Cyclin D1 gene, presumably through release of PNR transrepression, but TBX2 gene expression remained repressed (Figure 5A, lane 3). As it is believed that cyclin D1 gene expresses in proliferating retina neurons, whereas TBX2 expresses in differentiated retina (Sowden *et al*, 2001), Ret-CoR was presumed to function in developing retina.

We then directly tested the co-repressor function of Ret-CoR for PNR on PNR target gene promoters (Figure 5B) using

©2007 European Molecular Biology Organization

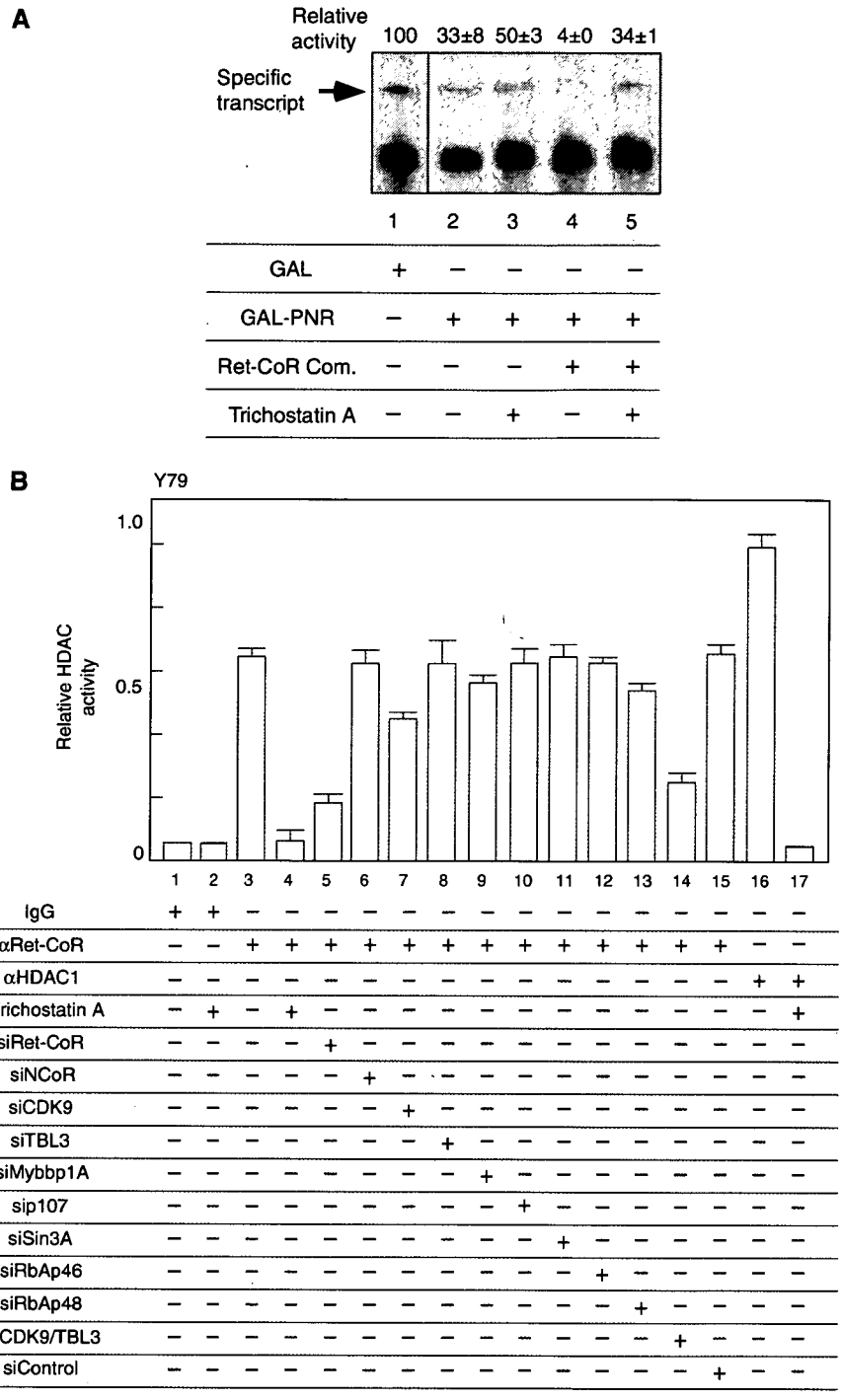

Figure 4 Characterization of the transcriptional repressive function of Ret-CoR containing complex. (**A**) Transrepressional ability of PNR and Ret-CoR were measured with the chromatinized histone octamers and the purified Ret-CoR complex (Figure 2B) by *in vitro* transcription assay. Each assay was performed with or without 500 nM Trichostatin A. (**B**) HDAC activity of a Ret-CoR immnoprecipitants from Y79. Asynchronized whole cell extracts were prepared and immunoprecipitated with either rabbit IgG antibody, anti-Ret-CoR antibody or anti-HDAC1 antibody. Immunoprecipitants were applied on an HDAC assay with or without 10^{-9} M Trichostatin A.

a luciferase reporter and ChIP assays in Y79 cells. The cyclin D1 gene appeared to harbor no putative, or related, PNR-binding sites in its promoter. However, together with a ChIP analysis (Figure 5C and D), functional analysis of promoter deletion mutants (Figure 5E) mapped a putative PNR target region similarly acting in the promoters (L-CycD1-luc and S-CycD1-luc) (see Figure 5B, upper panel). For the TBX2 promoter, recruitment of PNR, but not Ret-CoR, was observed (Figure 5C), which reflected the results of the repressor function experiments (Supplementary Figure 1C). Although PNR among NRs is closely related to TLX that is recently reported as a critical factor for development of neurons including retina (Zhang *et al*, 2006), TLX recruitment was not detected in the PNR target gene promoters (Figure 5C). Conversely, in a TLX target promoter (PTEN) (Zhang *et al*, 2006), neither PNR nor Ret-CoR was recruited (Figure 5C).

©2007 European Molecular Biology Organization

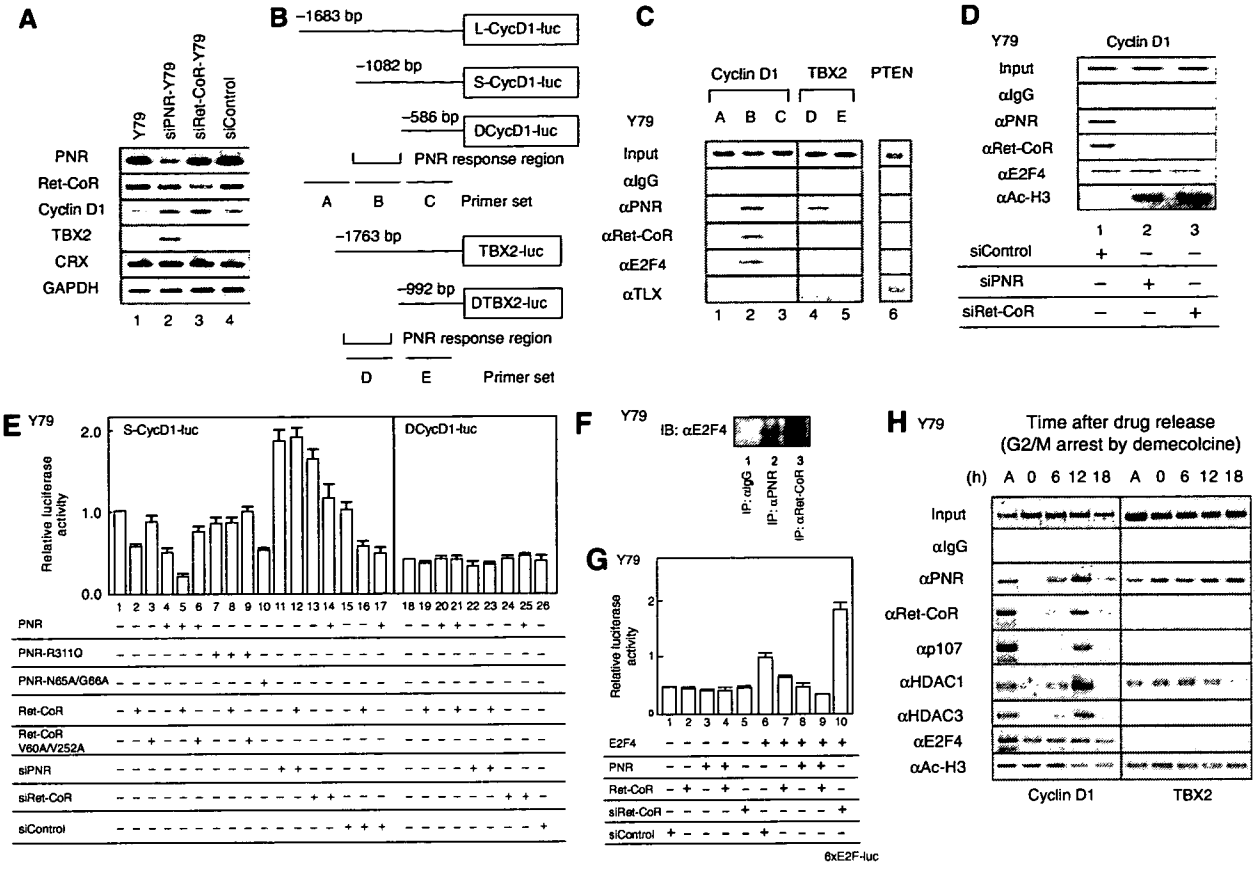

Figure 5 Promoter-specific function of the Ret-CoR containing complex. (**A**) The expression levels of the indicated genes were measured by RT–PCR with extracted total RNA from Y79, transfected with siPNR-Y79, siRet-CoR-Y79 or siControl. (**B**) Schematic diagrams of cyclin D1 promoter and TBX2 promoter with a putative PNR-binding element site. (**C**) ChIP assay was performed to endogenous Cyclin D1 promoter, TBX2 promoter and PTEN promoter with anti-IgG antibody, anti-PNR antibody, anti-Ret-CoR, anti-E2F4 and anti-TLX antibody. (**D**) ChIP assay was performed to Cyclin D1 promoter PNR responsive region (Cyclin D1-B) with anti-IgG antibody, anti-PNR antibody, anti-Ret-CoR antibody and anti-acetyl-Histone H3 treated with transfected siPNR, siRet-CoR or siControl. (**E**) Suppressive effects of PNR and Ret-CoR on Cyclin D1 promoter function. The functions of PNR-CyclinD1-luc (−1082 to 53 bp) or ΔCyclinD1 (−586 to 53 bp) luc promoters in a luciferase assay. (**F**) Co-immunoprecipitation of endogenous E2F4 with endogenous PNR and Ret-CoR. The immunocomplex was precipitated in Y79 cells with anti-PNR or Ret-CoR antibody and Western-blotted with anti-E2F4 antibody. (**G**) Ret-CoR co-represses transcriptional activity of E2F4 on the 6 × E2F response element-containing reporter. Luciferase assays were performed in Y79 cells transfected with 6 × E2F-luc reporter plasmids (400 ng), E2F4 expression vectors (200 ng), Ret-CoR expression vectors (100 ng) and double-stranded siRet-CoR or siControl (20 μM). (**H**) Cell cycle-dependent recruitment of Ret-CoR complex components to Cyclin D1 and TBX2 promoters. ChIP analysis was performed and synchronized Y79 cells at M phase and tested at an indicated time after drug release. Efficiency of synchronization of Y79 cells was determined by FACS as shown in Figure 3A.

A PNR mutant that lacked DNA-binding ability (PNR-N65A/G66A) still potently suppressed Cyclin D1 promoter function (Figure 5E). Notably, the repressive effect of PNR was attenuated by a PNR point mutation (R311Q) found in ESCS patients (Gerber *et al*, 2000; Haider *et al*, 2000), and by mutations in the CoRNR motif (V60A/V252A) of Ret-CoR (Figure 5E). No clear DNA binding of PNR was found in the Cyclin D1 gene promoter region by EMSA (data not shown). To explore further the molecular basis of the transrepressive function of PNR/Ret-CoR in the cyclin D1 gene promoter, we examined an idea if PNR/Ret-CoR associates with E2F family members, as the mapped PNR response element compromises DNA-binding sites for E2F family transcriptional regulators. This idea was further supported by the findings that the isolated Ret-CoR complex contains potential binding components for E2Fs (see Figure 2B). By co-immunoprecipitation, association of endogenous PNR and Ret-CoR proteins with endogenous E2F4 was detected (Figure 5F). Co-repression of E2F4 transcriptional activity by Ret-CoR/PNR was seen in the Cyclin D promoter (L-CycD1-luc) (data not shown) and in the synthetic E2F-binding sites (Figure 5G). Consistent with these findings, recruitment of E2F4 to the promoter Cyclin D, was detectable (Figures 5C, D and H). Moreover, cell cycle-dependent recruitment of PNR and Ret-CoR complex components to regulatory regions in the Cyclin D1 gene promoter was detected by ChIP analysis (Figure 5H). However, for the TBX2 gene promoter, recruitment of PNR, but not Ret-CoR, was observed (Figure 5H). Thus, taken together, our findings suggested that the transrepressive function of PNR in the developing retina requires the co-repressor function of Ret-CoR, presumably as an HDAC complex, with cell cycle-dependent appearance.

Cyclin D1 and TBX2 gene expression is under negative control by PNR in the developing retina

Finally, to address the physiological significance of the observed findings *in vitro*, we measured the expression of PNR and Ret-CoR in the developing retina. Although high PNR and

©2007 European Molecular Biology Organization

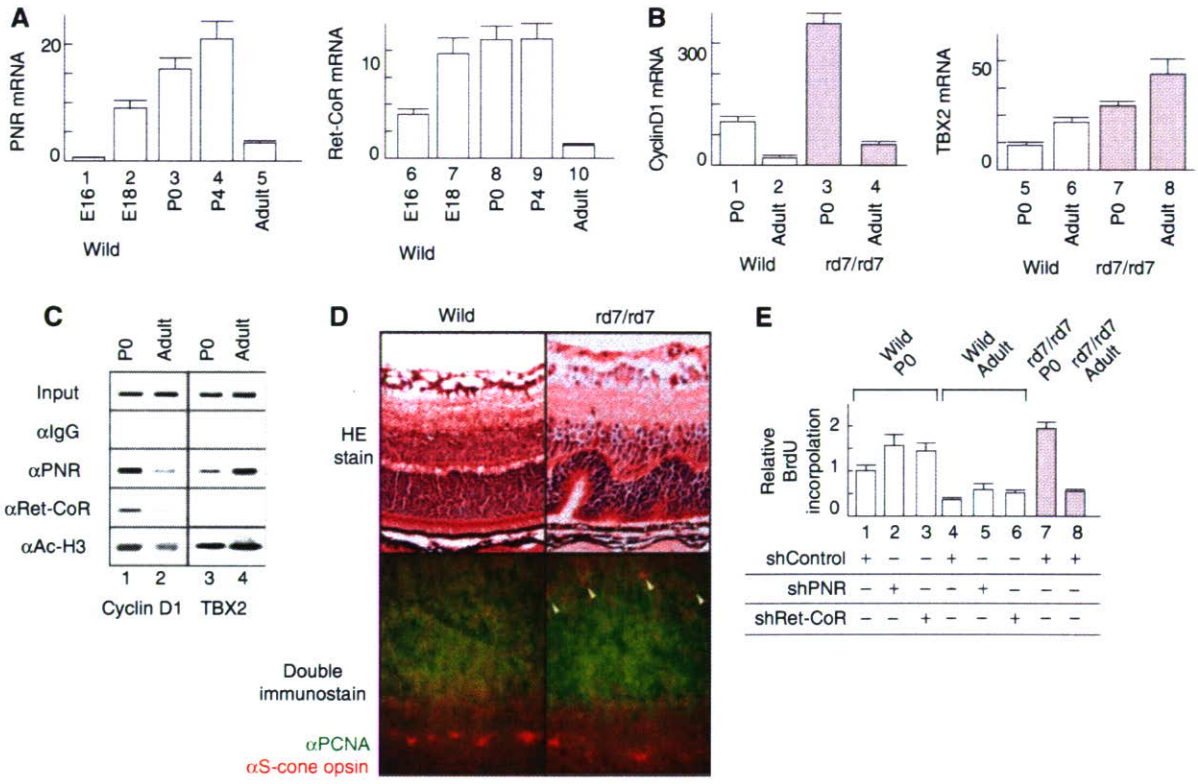

Figure 6 Expression profiles of PNR, Ret-CoR and their target genes during retinal development. (**A**) Transcript levels of the mouse retina at embryonic day 16 to postnatal day 4 and adult phase were quantified by real-time PCR. (**B**) Increased expression of Cyclin D1 and TBX2 as putative PNR/Ret-CoR complex target genes in the retina of wild mice or rd7/rd7 mice quantified by real-time PCR. (**C**) Cyclin D1 and TBX2 promoter occupancy of PNR and Ret-CoR in the mice retina was showed by *in vivo* ChIP assay. (**D**) Hyperproliferation of the retinal progenitor cells. The retina of the wild mice and rd7/rd7 mice at postnatal day 5 were stained with hematoxylin and eosin (upper panel). Rossett formation in the rd7/rd7 mice suggests hyperproliferated S-cone cells from retinal progenitor cells. Sections of developing retinas of wild-type and rd7/rd7 mice at P0 were double-immunostained with as 'green' for PCNA, a marker for dividing retinal progenitor cells and as 'red' for S-cone opsin (lower panel). (**E**) Dissociated retina of the wild mice and rd7/rd7 mice at postnatal day 0- and 12-week old were cultured and incorporated BrdU. Retro virus of control-shRNA (shControl), shPNR or shRet-CoR was infected, respectively.

Ret-CoR expression levels were observed in developing retinas from wild-type mice from stages E18 to P4, only low levels were observed in the mature retina of adult mice (Figure 6A). Further suggestive of the repressor function of PNR, clear upregulation of Cyclin D1 and TBX2 gene expression was observed in the developing retina of mice that lacked functional PNR (rd7/rd7, a spontaneous PNR gene mutant line) (Figure 6B). However, in the retina of adult rd7/rd7 mice, upregulation of the TBX gene, but not the cyclin D1 gene, was observed, which suggested a developmental stage-specific function for PNR through interaction with multiple co-repressor complexes in the retina (see Figure 7). Indeed, by *in vivo* ChIP analysis, a clear Ret-CoR recruitment to the Cyclin D1 gene promoters was detected in the developing retina of P0 mice, rather than in the mature retina of adult mice (Figure 6C). As previously reported in mice and human ESCS patients (Akhmedov *et al*, 2000; Gerber *et al*, 2000; Haider *et al*, 2000), an increased number of S-cone cells with normal M-cone cell number was reported from the retina of rd7/rd7 mice (see upper panel in Figure 6D). In the retina of the wild-type mice at P0, S-cone opsin (stained as red) expression was not detected in the layers of PCNA-positive dividing cells (green), confirming that at P0 stage, no proliferation of the S-cone progenitor cells. However, in the retina of rd7/rd7 mice, S-cone opsin expression was detectable in the layers of PCNA-positive dividing cells (see arrowheads in lower panels in Figure 6D), suggesting that S-cone progenitor cells are still proliferating at P0. Such PNR function in retina development was then examined in embryonic retina cells (Figure 6E). Knockdown of PNR with a retrovirus (Supplementary Figure 1B) appeared to induce cell proliferation, as seen in hyperproliferative retina cells derived from rd7/rd7 mice at P0, supporting the putative PNR suppressive function for retina cell proliferation. Thus, Ret-CoR co-repressor function, presumably as an HDAC complex, appears to be required for PNR function in retinal progenitor cells, but not in differentiated retinal cells (Figure 7).

Discussion

The role of Ret-CoR function in retina development

PNR is known to serve as a negative regulator for cell proliferation of retina neurons. As established in ESCS patients and rd7/rd7 mice, S-cone cell proliferation appears under a negative control by PNR, whereas differentiation switching of S-cone cells into M-cone cells appears to require the other factors (Haider *et al*, 2001; Milam *et al*, 2002; Yanagi *et al*, 2002). The molecular mechanism of suppression of S-cone cell proliferation by PNR still remains elusive, but PNR-mediated transcriptional repression of genes involving cell-cycle regulation has been already revealed (Yanagi *et al*, 2002). Together with the present findings that the Ret-CoR

©2007 European Molecular Biology Organization